NATIONAL ADVISORY COMMITTEE FOR AERONAUTICS

TECHNICAL NOTE

No. 1191

TWO-DIMENSIONAL WIND-TUNNEL INVESTIGATION OF FOUR TYPES OF HIGH-LIFT FLAP ON AN NACA 65-210 AIRFOIL SECTION

By Jones F. Cahill

Langley Memorial Aeronautical Laboratory
Langley Field, Va.

Washington
February 1947

NATIONAL ADVISORY COMMITTEE FOR AERONAUTICS

TECHNICAL NOTE NO. 1191

TWO-DIMENSIONAL WIND-TUNNEL INVESTIGATION OF FOUR TYPES OF HIGH-LIFT FLAP ON AN NACA 65-210 AIRFOIL SECTION

By Jones F. Cahill

SUMMARY

An investigation was made in the Langley two-dimensional low-turbulence tunnels to develop flap configurations for maximum lift of the NACA 65-210 airfoil section equipped with four types of high-lift flap. Lift and pitching-moment data were obtained for the optimum configurations. Scale effect and the effect of standard leading-edge roughness an maximum lift coefficient were also determined.

Tests were made of three 25-percent-chord single slotted flaps with the trailing edges of the slot lips located at 84, 90, and 97.5 percent of the airfoil chord, and of a 31.2-percent-chord double slotted flap. For the model with each of the flaps, the maximum lift was shown to become more sensitive to small movements of the flap as the flap deflection was increased. The maximum lift coefficient of the airfoil with each of the single slotted flaps was shown to be about 2.47 and that with the double slotted flap was 2.73 at a Reynolds number of 6×10^6. The maximum lift coefficient was shown to increase as the Reynolds number was increased in the range of Reynolds number from 2 to 4 or 6×10^6, but in some cases the maximum lift coefficient decreased at higher Reynolds numbers. The decrement in maximum lift caused by standard roughness decreased as the flap deflection was increased and at the higher deflections was approximately the same as the decrement obtained with the plain airfoil.

INTRODUCTION

An extensive investigation of thin airfoil sections has been undertaken by the National Advisory Committee for Aeronautics to obtain information applicable to the design of high-speed airplanes. Since very little data for flaps on thin NACA 6-series airfoil

sections are available, tests were made of an NACA 65-210 airfoil section equipped with four types of high-lift flap.

The NACA 65-210 airfoil section was believed to offer a reasonable compromise between high maximum lifts and high critical speeds. The greatest amount of data available on the application of high-lift flaps to fairly thin airfoil sections has been obtained from tests of the NACA 23012 airfoil. Data on this airfoil with various types of flap have been presented in references 1, 2, and 3. These data were obtained with a simple slotted flap, two slotted flaps with slot lips extended to 90 and 100 percent of the airfoil chord, and a double slotted flap. Reference 2 shows that the maximum lift and the pitching-moment increment obtained with single slotted flaps increase as the length of the slot lip is increased. The double slotted flap of reference 3 produced maximum lifts about the same as the slotted flap with the longest slot lip (Fowler flap) and pitching-moment increments about the same as the single slotted flap with the 90-percent-chord lip extension. The use of long slot-lip extensions presents structural problems that are accentuated by the very thin rear parts of the present NACA 6-series sections. The flaps used in the present investigation were designed to provide as much thickness for structure in the slot lip as was considered compatible with reasonable flap thicknesses.

The present paper covers an investigation in the Langley two-dimensional low-turbulence tunnels of a series of slotted flaps similar to the flaps of references 1 to 3. Tests were made to develop optimum flap configurations for maximum lift of three slotted flaps with varying slot-lip extensions and of a double slotted flap. Scale effect, the effect of roughness on lift characteristics, and pitching-moment characteristics with the flaps deflected were also determined.

SYMBOLS

α_o	section angle of attack
c	basic airfoil chord
c_l	section lift coefficient
$c_{l_{max}}$	maximum section lift coefficient

$c_{m_{c/4}}$	section pitching-moment coefficient about quarter-chord point
Δc_l	increment of section lift coefficient
$\Delta c_{l_{max}}$	increment of maximum section lift coefficient
$\Delta c_{m_{c/4}}$	increment of section pitching-moment coefficient about quarter-chord point
x, y	horizontal and vertical positions, respectively, of flap reference point measured from most rearward station of slot lip in percent of c (x positive forward and y positive below)
x_1, y_1	positions of fore-flap reference point
x_2, y_2	positions of main-flap reference point measured from trailing edge of fore flap
δ_f	deflection of flap, measured between flap chord line when flap is deflected and flap chord line when flap is retracted
δ_{ff}	deflection of fore flap, measured from wing chord line
R	Reynolds number

MODELS

The basic airfoil used in the present tests had a chord of 2 feet and completely spanned the 3-foot-wide test sections of the tunnels. The main part of the model ahead of the flaps was constructed of mahogany and was provided with detachable trailing-edge pieces for each of the flaps.

The flaps were constructed of steel and each of the single slotted flaps had a chord of 25 percent of the basic airfoil chord. The single slotted flaps are designated slotted flaps 1, 2, and 3 and were designed with the trailing edge of the slot lip at 84, 90, and 97.5 percent of the basic airfoil chord, respectively. These flaps had thicknesses of 14.16, 11.56, and 8.92 percent of the flap chord, respectively. Slotted flap 1 was used as the main-flap part of the double slotted flap. The fore flap had a chord of 7.5 percent of the basic airfoil chord. The final configuration of the fore flap

and the main flap was such that the two flaps could be deflected as a unit and enclosed within the airfoil profile when retracted. The total length of the combination in this configuration was 31.2 percent of the basic airfoil chord. Ordinates of the airfoil section and of the flaps are given in table I and sketches of the various flaps in retracted and extended positions are shown in figure 1.

The flaps were attached to the main part of the airfoil by fittings at the ends that permitted any desired position or deflection. For the double slotted flap, the fore flap and the main flap were mounted so that each flap could be moved independently until an optimum position of the main flap with respect to the fore flap was developed at the 50° deflection and then the two flaps were attached rigidly together. Configurations of the flaps are defined by the positions of their reference points and their deflections as shown in figure 1(b). The reference points are defined as the intersection of the flap chord lines and the contour of the flap nose. Deflections were measured between the flap chord line when the flap was retracted and the flap chord line when the flap was deflected. When the double slotted flap was tested as a unit, the deflection was defined by the deflection of the main flap and the fore-flap reference point was used to define the position.

For the normal smooth condition, the model was finished with No. 400 carborundum paper to produce aerodynamically smooth surfaces. For the standard leading-edge roughness condition, the model surfaces were the same as in the smooth condition, but 0.011-inch carborundum grains were applied to the leading edge over a surface length of 0.08c measured from the leading edge on each surface. The roughness applied corresponds to the definition of standard roughness given in reference 4.

TESTS

Preliminary tests of the model with each of the flaps were first conducted at a Reynolds number of 2.4×10^6 for the purpose of determining the optimum configuration of each flap for maximum lift. Lift readings were taken over the peak of the lift curve for a number of flap positions at several flap deflections. In each case enough positions were investigated to ensure the choice of optimum position and to show the effect of deviations from the optimum configuration. Because of the large number of tests involved in determining an absolute optimum configuration of the double slotted flap, the fore-flap and main-flap deflections were set at 25° and 50°, respectively, and an optimum position

of the main flap with respect to the fore flap was developed. Optimum positions of the fore flap and main flap as a unit were then developed for several flap deflections with the main flap and fore flap held at this relative position.

Lift data at Reynolds numbers of 2.4 and 6.0×10^6, pitching-moment data, and data on the effect of standard leading-edge roughness were determined at the optimum configuration for each flap deflection for slotted flaps 1 and 2 and for the double slotted flap, and the scale effect on maximum lift was investigated at one deflection near the deflection for maximum lift.

Tests of the model with slotted flap 3 were discontinued after a few tests showed that the maximum lifts produced by use of this flap were no higher than the maximum lifts produced by use of slotted flaps 1 and 2.

All lift measurements were made by the methods described in reference 4 and were corrected to free-air values according to the equations given in the appendix of reference 4.

PRESENTATION OF RESULTS

Lift and pitching-moment data for the plain airfoil from reference 4 are shown in figure 2. Lift data are also shown for the model with a 0.20c simulated split flap deflected 60° for several Reynolds numbers.

Contours of flap position for maximum lift at several deflections for each of the flaps are shown in figures 3 to 7. In each figure the flap is drawn in at the position at which the highest maximum lift was measured. Figure 3 shows the contour of values of maximum lift coefficient for main-flap positions with respect to the fore-flap trailing edge. Contours of values of maximum lift coefficient for positions of the main flap and fore flap as a unit at various deflections are presented in figure 4. Figures 5, 6, and 7 show contours obtained for various deflections of slotted flaps 1, 2, and 3, respectively.

The data shown in figures 8 to 18, with the exception of data for slotted flap 3, include lift characteristics for the model in both the smooth and the standard leading-edge roughness conditions, pitching-moment data and scale-effect data on lift characteristics. For slotted flap 3, only the lift characteristics at a Reynolds number of 2.4×10^6 and the scale-effect data were

obtained. These data showed that the maximum lifts obtained with flap 3 were no higher than the maximum lifts obtained with slotted flaps 1 or 2. Since construction of a flap similar to slotted flap 3 presents greater problems than construction of slotted flaps 1 and 2, the tests of slotted flap 3 were discontinued.

DISCUSSION

Optimum Configurations for Maximum Lift

In nearly all cases the contours show that, at the optimum maximum lift position, the gap between the slot lip and the flap nose is slightly decreased as the flap deflection is increased. In all cases, the flaps are shown to be more sensitive to slight changes in position as the deflection is increased. The contours show the necessity for care in locating the main flap and the fore flap and in maintaining tolerances in construction. For example, in figure 4(e), a change of 1 percent of the wing chord from the optimum position can cause a decrease of 16 percent in the value of the maximum lift coefficient.

Scale Effect

Values of the maximum lift coefficient are plotted in figure 19 against Reynolds number for each of the flaps. The maximum lift of the airfoil with each of the flaps is shown to increase as the Reynolds number is increased from 2 to 4 or 6×10^6, but this effect decreases as the Reynolds number is increased above 4 or 6×10^6. The data for the model with the split flap deflected 60° show a similar scale effect but decidedly lower maximum lifts. Throughout the range of Reynolds number tested the maximum lift coefficient of the plain airfoil increases as the Reynolds number is increased. Figures 9, 12, 15, and 18 show that at the higher Reynolds numbers the lift curves at low angles of attack are shifted downward. Tests were made at several different values of the dynamic pressure at a Reynolds number of 6×10^6 (by varying the tunnel pressure) and the results indicated that this downward shift of the lift curves was not caused by deflections of the model. The optimum position found at a Reynolds number of 2.4×10^6 might not be the optimum at the higher Reynolds numbers.

Effect of Roughness

Curves are presented in figure 20 that show the decrement in maximum lift coefficient caused by the addition of standard roughness to the airfoil leading edge at various deflections of three of the flaps. In all cases shown the effect of roughness on maximum lift decreases with an increase in flap deflection and at the higher deflections is approximately the same as the effect obtained from tests of the plain airfoil. Figures 8(c), 11(c), and 14(c) show that, at high flap deflections, the lift coefficients increase sharply up to the maximum lift in the leading-edge roughness condition. Tuft studies showed that the flow over the flap was rough in the intermediate range of lift coefficient in both the smooth and the rough conditions and that in the rough condition the flow over the flap improved before the main part of the wing stalled. No such improvement was noted in the smooth condition. This effect is noticed in the data obtained with each of the flaps but is very slight with the double slotted flap. For tests in the smooth condition the model was kept very smooth and accurately to contour. The discussion of the lift characteristics of rough airfoils contained in reference 4 may be applied to these results.

Pitching Moments

Increments of pitching-moment coefficient are plotted against increments of lift coefficient at an angle of attack of 0° in figure 21. The relation between these increments is shown to be almost linear; this fact indicates that the incremental load distribution caused by deflection of the flap remains constant in shape for various deflections and depends only on the value of incremental lift coefficient.

Comparison of Flaps

Values of the maximum lifts are plotted against flap deflection in figure 22 for slotted flaps 1 and 2 and the double slotted flap. The highest maximum lift coefficients measured were 2.47, 2.48, and 2.46 with slotted flaps 1, 2, and 3, respectively, and 2.73 with the double slotted flap. The double slotted flap is shown to produce the highest maximum lifts in both the smooth and the rough conditions. The maximum lift of the model with the double slotted flap with the leading-edge roughness is only slightly lower than the maximum lift of the model with the other flaps in the smooth condition.

Despite the large increases in area obtained when slotted flaps 2 and 3 are deflected, the maximum lift of the model with these flaps was no higher than the maximum lift with slotted flap 1. The small leading-edge radii of slotted flaps 2 and 3 are believed to be responsible for the comparatively low maximum lifts.

The pitching-moment increments presented in figure 21 show that the pitching-moment increment for a constant lift increment increases as the length to which the flap extends is increased. The increments for the double slotted flap are shown to be approximately equal to the increments for slotted flap 2. The total chord, or flap chord plus airfoil chord (to the end of the slot lip), is the same for these two flaps. The decrease in airplane lift coefficient caused by the down load on the tail required to trim the wing pitching moment is also shown in figure 21. This down load was calculated from the equation

$$\Delta c_{l_t} = \frac{c_{m_{c/4}}}{l_t}$$

where

Δc_{l_t} decrease in lift coefficient caused by down load on tail

l_t tail length in airfoil chords

This equation is not exact since variations in downwash at the tail are ignored; however, the accuracy is sufficient to show a comparison among the various types of flap. Although the pitching moments are considerably higher for the double slotted flap than for slotted flap 1, the difference in the trim loads is not great enough to change the relative effectiveness of the two flaps.

CONCLUSIONS

A 24-inch-chord model of the NACA 65-210 airfoil section equipped with three single slotted flaps having various slot-lip extensions and with a double slotted flap was tested in the Langley two-dimensional low-turbulence tunnels to develop flap configurations for maximum lift. The results of the tests indicated the following conclusions:

1. The maximum lift coefficient of the model with each of the single slotted flaps was about 2.47 and with the double slotted flap was 2.73 at a Reynolds number of 6×10^6.

2. As the flap deflection was increased, the optimum position of the flap became closer to the upper slot lip and the sensitivity of the maximum lift to small movements of the flap increased.

3. In all cases tested, the maximum lift coefficient was increased by increases in Reynolds number in the range of Reynolds number from 2×10^6 to 4 or 6×10^6, but in some cases the maximum lift coefficient decreased at values of the Reynolds number above 4 or 6×10^6.

4. The decrement in maximum lift caused by standard roughness decreased as the flap deflection was increased and at the higher deflections was approximately the same as the decrement obtained with the plain airfoil.

5. Pitching-moment increments caused by flap deflection were higher at a constant value of lift increment for the double slotted flap than for the single slotted flap with the shortest slot-lip extension but were approximately equal to the pitching-moment increments for the single slotted flap with the intermediate slot-lip extension. The loss in lift coefficient caused by trimming loads on the tail did not change the relative effectiveness of the flaps.

Langley Memorial Aeronautical Laboratory
National Advisory Committee for Aeronautics
Langley Field, Va., September 5, 1946

REFERENCES

1. Wenzinger, Carl J., and Harris, Thomas A.: Wind-Tunnel Investigation of an N.A.C.A. 23012 Airfoil with Various Arrangements of Slotted Flaps. NACA Rep. No. 664, 1939.

2. Lowry, John G.: Wind-Tunnel Investigation of an NACA 23012 Airfoil with Several Arrangements of Slotted Flaps with Extended Lips. NACA TN No. 808, 1941.

3. Purser, Paul E., Fischel, Jack, and Riebe, John M.: Wind-Tunnel Investigation of an NACA 23012 Airfoil with a 0.30-Airfoil-Chord Double Slotted Flap. NACA ARR No. 3L10, 1943.

4. Abbott, Ira H., von Doenhoff, Albert E., and Stivers, Louis S., Jr.: Summary of Airfoil Data. NACA ACR No. L5C05, 1945.

TABLE I.- ORDINATES FOR AIRFOIL AND FLAPS

[All dimensions in percent of basic airfoil chord]

NACA 65-210 airfoil

Upper surface		Lower surface	
Station	Ordinate	Station	Ordinate
0	0	0	0
.435	.819	.565	-.719
.678	.999	.822	-.859
1.169	1.273	1.331	-1.059
2.408	1.757	2.592	-1.385
4.898	2.491	5.102	-1.859
7.394	3.069	7.606	-2.221
9.894	3.555	10.106	-2.521
14.899	4.338	15.101	-2.992
19.909	4.938	20.091	-3.346
24.921	5.397	25.079	-3.607
29.936	5.732	30.064	-3.788
34.951	5.954	35.049	-3.894
39.968	6.067	40.032	-3.925
44.984	6.058	45.016	-3.868
50.000	5.918	50.000	-3.709
55.014	5.625	54.986	-3.435
60.027	5.217	59.973	-3.075
65.036	4.712	64.964	-2.652
70.043	4.128	69.957	-2.184
75.045	3.479	74.955	-1.689
80.044	2.783	79.956	-1.191
85.038	2.057	84.962	-.711
90.028	1.327	89.972	-.293
95.014	.622	94.986	.010
100.000	0	100.000	0

L.E. Radius: 0.687
Slope of radius through L.E.: 0.084

Slotted flap 1

Upper surface		Lower surface	
Station	Ordinate	Station	Ordinate
0	0	0	0
.28	.92	.28	-.41
.56	1.19	.56	-.62
1.12	1.56	1.12	-.88
1.69	1.80	1.69	-1.00
2.25	1.99	2.48	-1.03
3.38	2.22	4.98	-0.83
4.50	2.33	7.48	-.63
5.61	2.38	9.98	-.44
7.00	2.40	12.48	-.27
9.00	2.35	14.98	-.12
11.00	2.16	17.48	.01
12.51	1.91	19.99	.10
15.01	1.50	22.49	.12
17.51	1.10	25.00	0
20.00	.71		
22.50	.34		
25.00	0		

L.E. Radius: 0.80
Slope of radius through L.E.: 0.35

Slotted flap 2

Upper surface		Lower surface	
Station	Ordinate	Station	Ordinate
0	0	0	0
.31	.67	.31	-.36
.62	.90	.62	-.50
1.25	1.23	1.25	-.64
1.88	1.45	1.88	-.69
2.50	1.61	2.50	-.70
3.75	1.80	3.75	-.65
5.00	1.92	5.00	-.56
6.25	1.96	7.50	-.40
7.50	2.00	9.99	-.24
10.00	1.95	12.49	-.10
12.50	1.82	14.99	.02
15.00	1.55	17.48	.11
17.50	1.20	19.99	.17
20.00	.78	22.49	.15
22.50	.38	25.00	0
25.00	0		

L.E. Radius: 0.40
Slope of radius through L.E.: 0.35

Slotted flap 3

Upper surface		Lower surface	
Station	Ordinate	Station	Ordinate
0	0	0	0
.31	.51	.31	-.24
.62	.71	.62	-.32
1.25	.98	1.25	-.42
1.88	1.18	1.88	-.45
2.50	1.32	2.54	-.45
3.75	1.46	5.03	-.31
5.00	1.52	7.52	-.17
6.25	1.53	10.01	-.05
7.50	1.51	12.50	.06
10.00	1.42	15.00	.15
12.50	1.27	17.49	.21
15.00	1.08	19.99	.23
17.50	.86	22.49	.18
20.00	.60	25.00	0
22.50	.33		
23.75	.18		
25.00	0		

L.E. Radius: 0.22
Slope of radius through L.E.: 0.34

NATIONAL ADVISORY
COMMITTEE FOR AERONAUTICS

Fore flap

Station	Upper ordinate	Lower ordinate
0	0	0
.42	.95	-.93
.83	1.31	-1.14
1.25	1.52	-1.20
1.67	1.62	-1.11
2.08	1.72	-.85
2.92	1.74	-.36
3.75	1.64	-.02
4.58	1.43	.18
5.42	1.13	.27
6.25	.75	.25
7.08	.28	.11
7.50	0	0

L.E. Radius: 1.20
(on chord line)

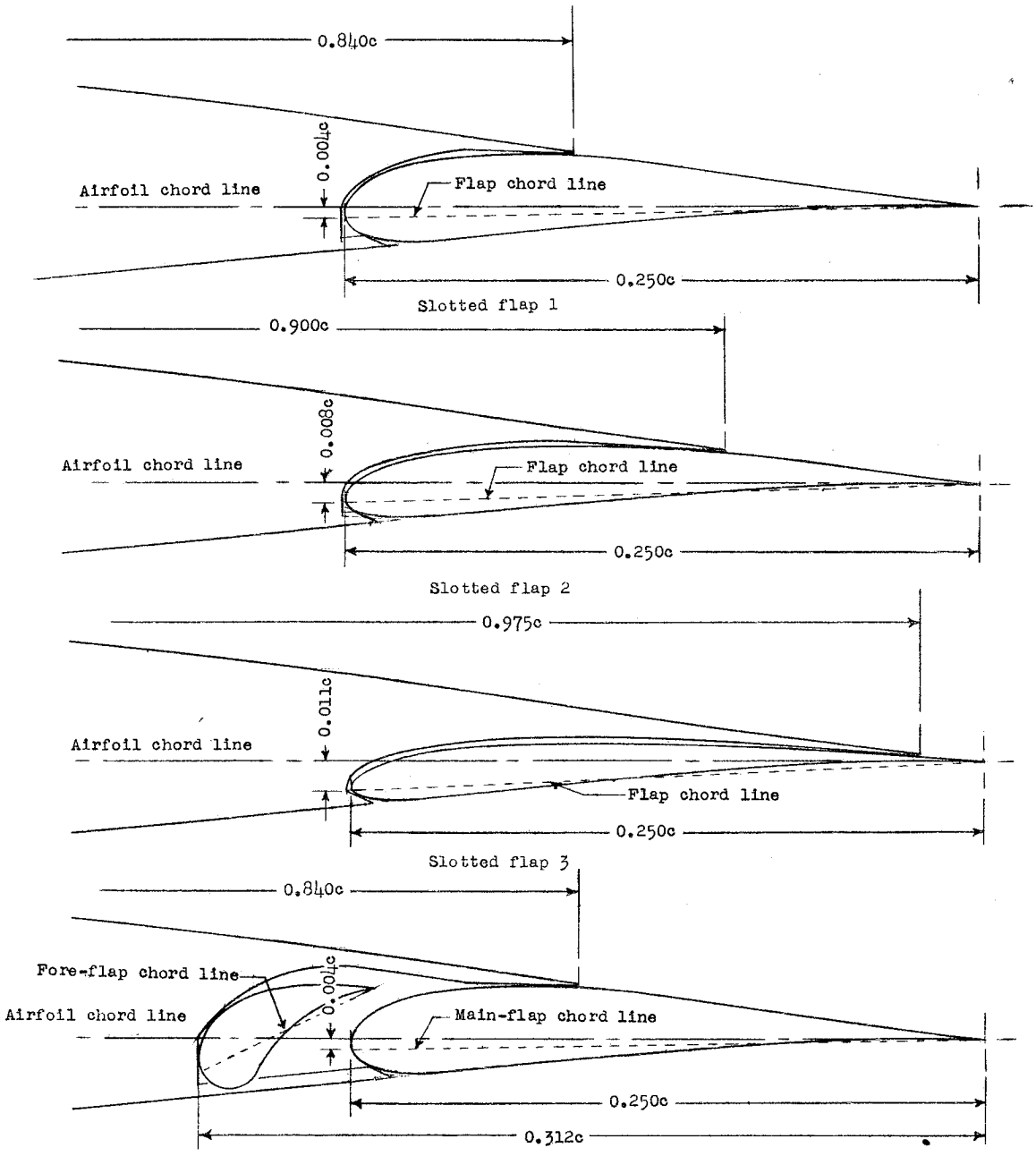

(a) Flaps tested.

Figure 1.- Sketch of flaps tested on NACA 65-210 airfoil section.

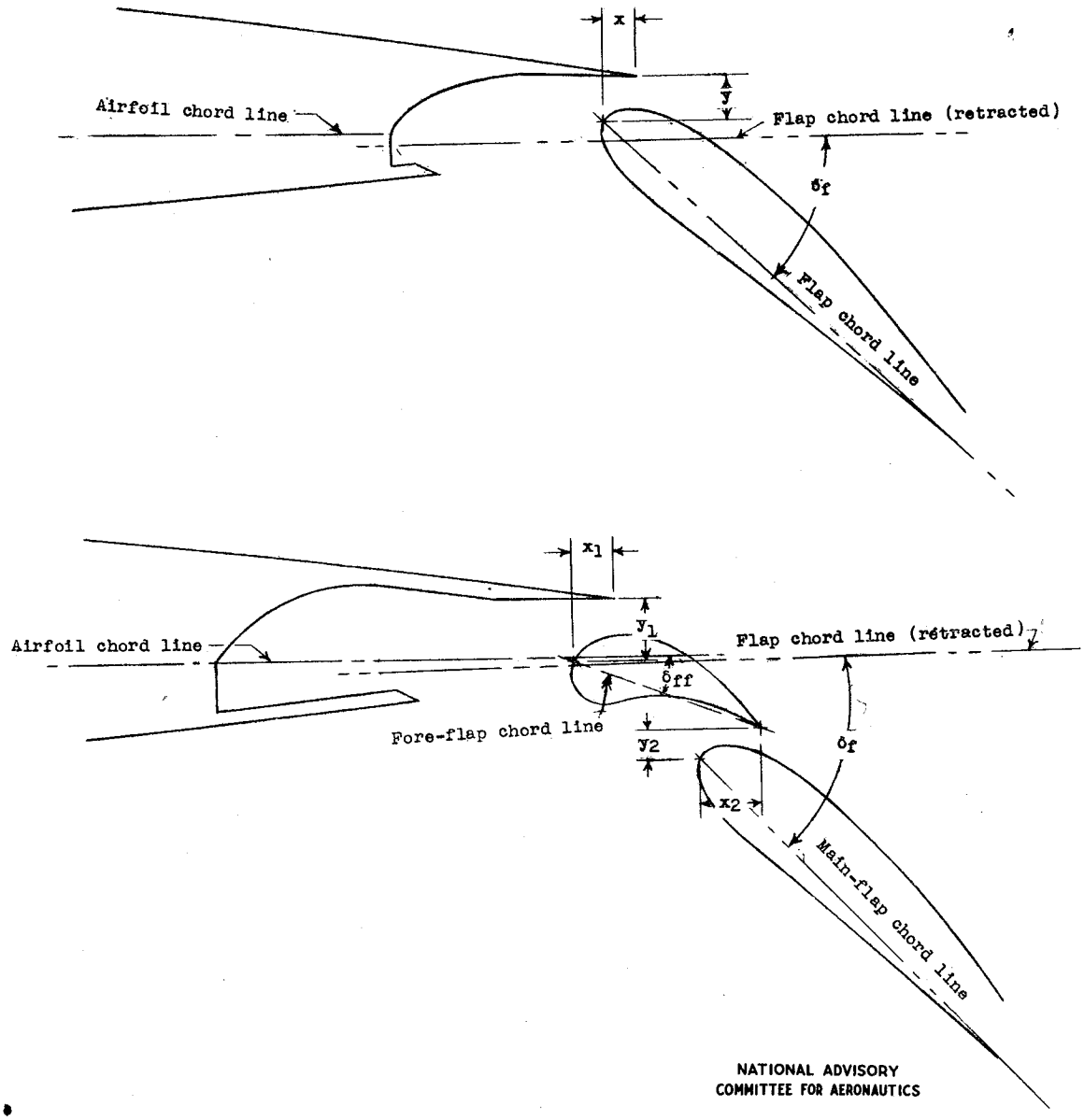

(b) Variables used to define flap configurations.

Figure 1.- Concluded.

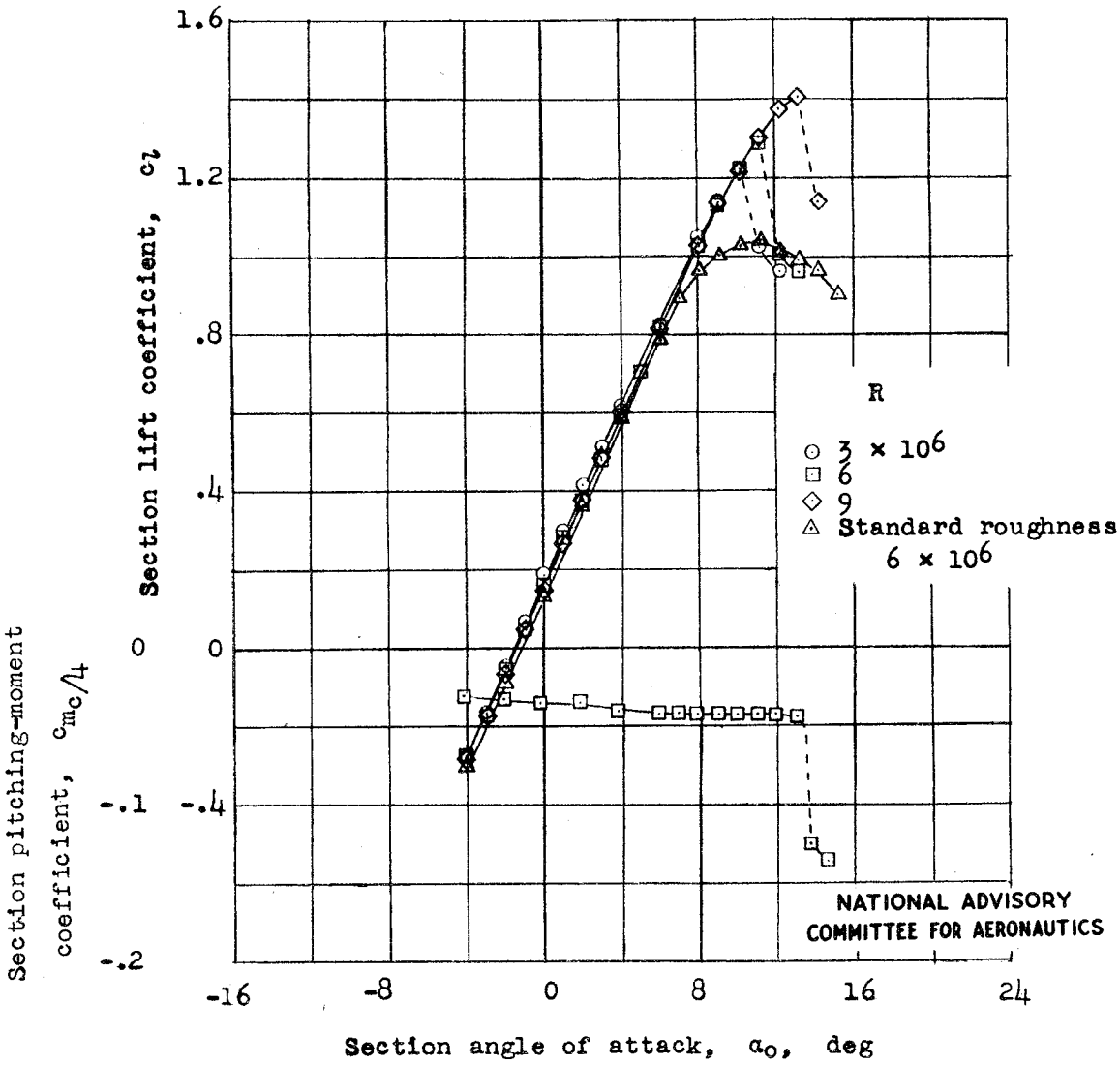

(a) Plain airfoil.

Figure 2.- Section lift and pitching-moment characteristics of the NACA 65-210 airfoil section. (Reference 4.)

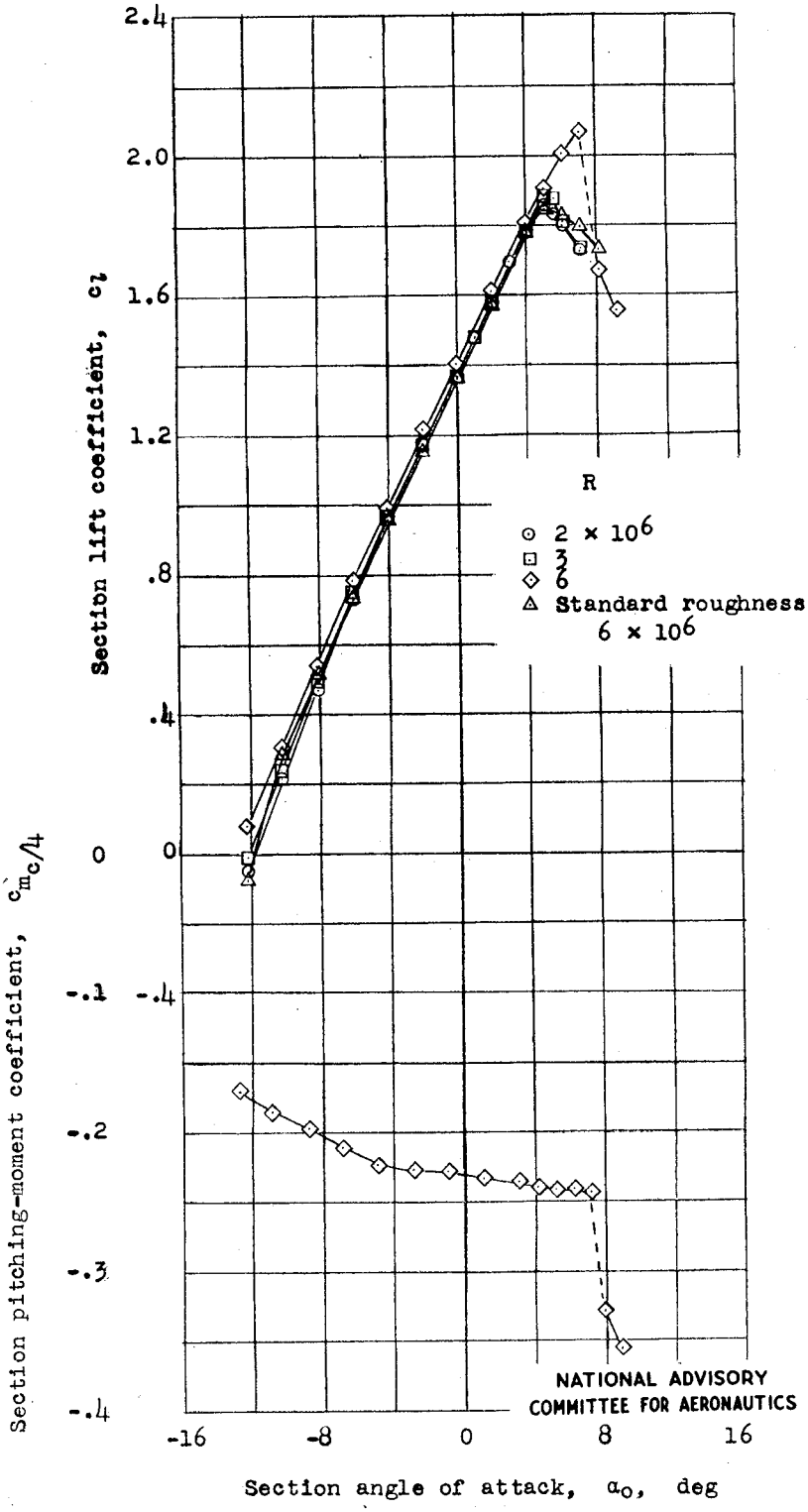

(b) Airfoil with 0.20c split flap. $\delta_f = 60^\circ$.

Figure 2.- Concluded.

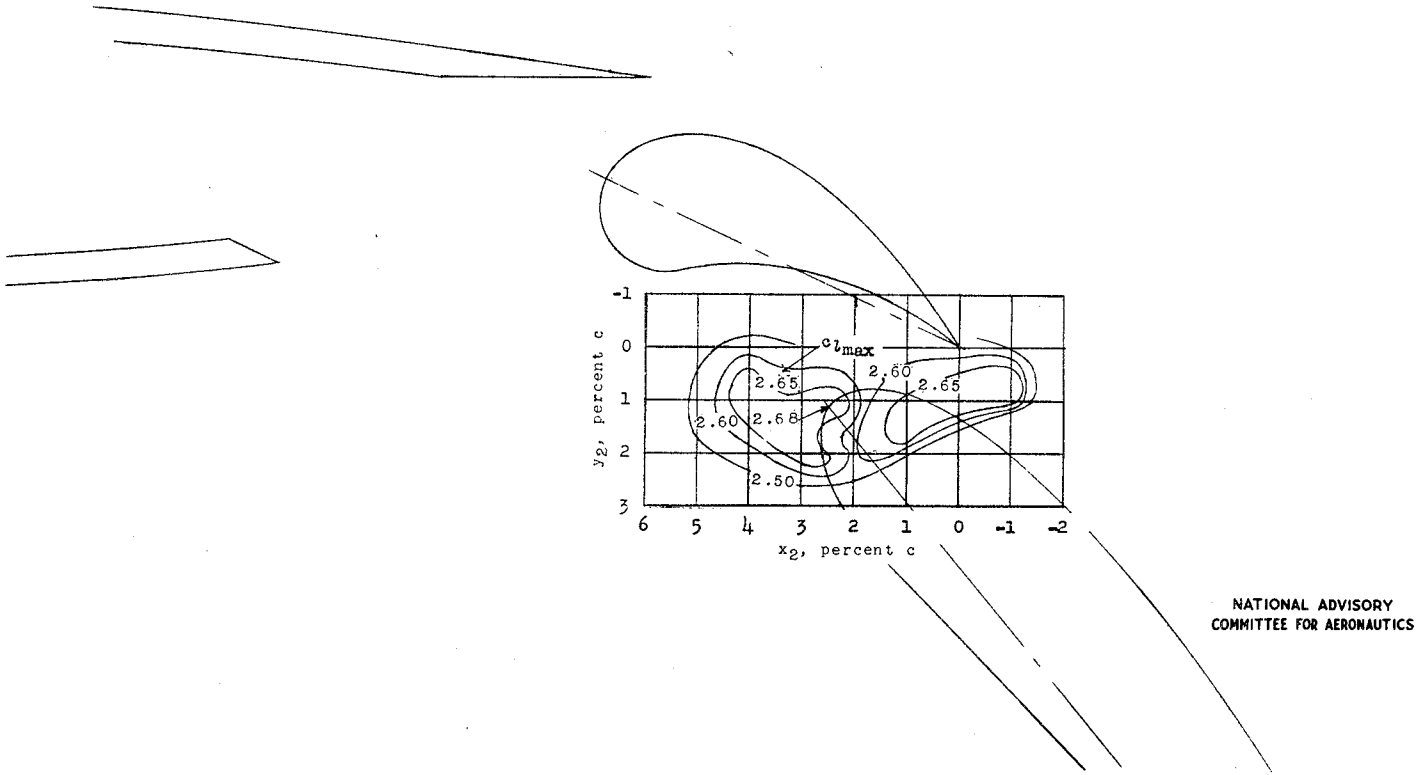

Figure 3.- Contours of values of maximum lift coefficient for main-flap positions with respect to fore-flap trailing edge. Double slotted flap; NACA 65-210 airfoil; $R = 2.4 \times 10^6$ (approx.); $\delta_{ff} = 25^\circ$; $x_1 = 0.9$; $y_1 = 1.9$; $\delta_f = 50^\circ$.

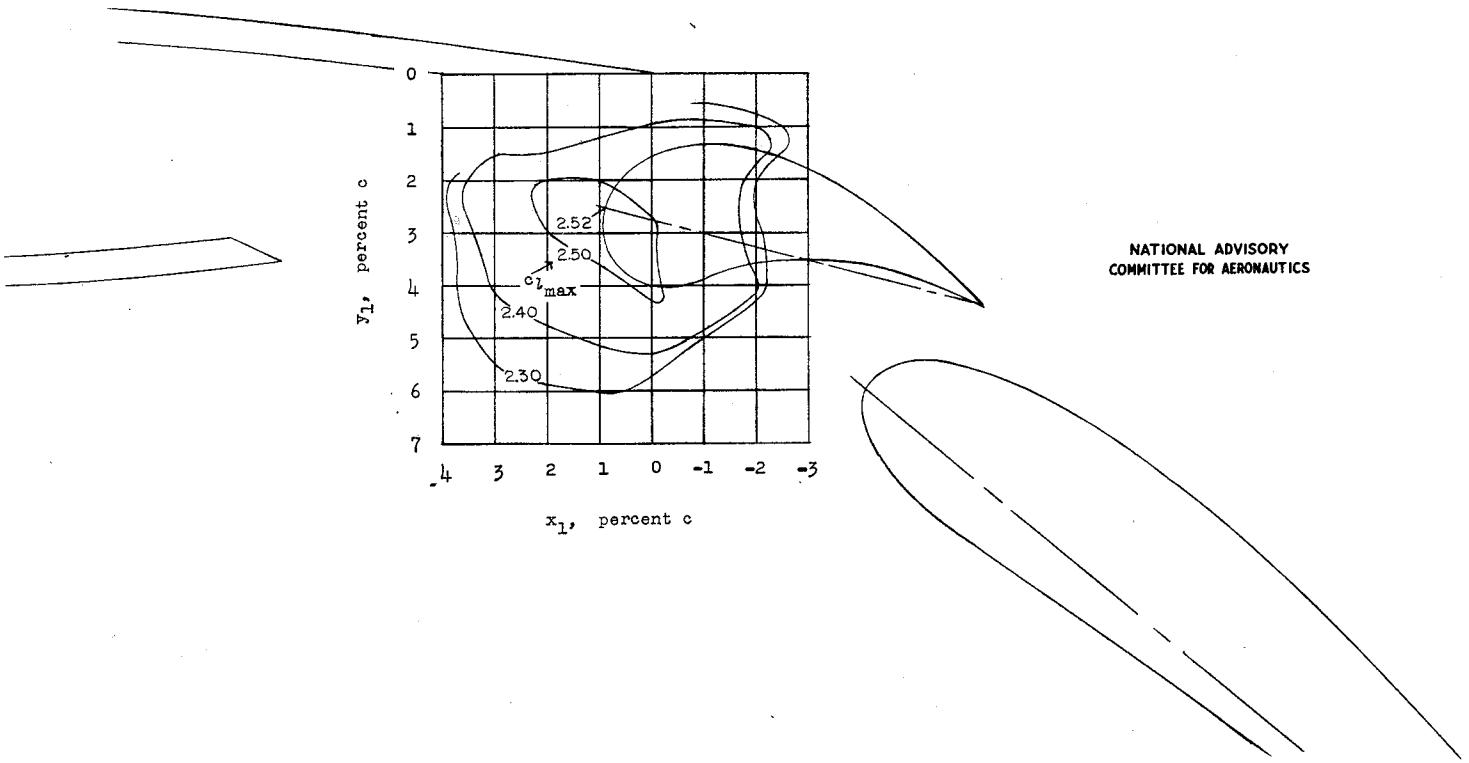

(a) $\delta_f = 40^\circ$.

Figure 4.- Contours of values of maximum lift coefficient for positions of main flap and fore flap as a unit at various flap deflections. 0.312c double slotted flap; NACA 65-210 airfoil; $R = 2.4 \times 10^6$ (approx.).

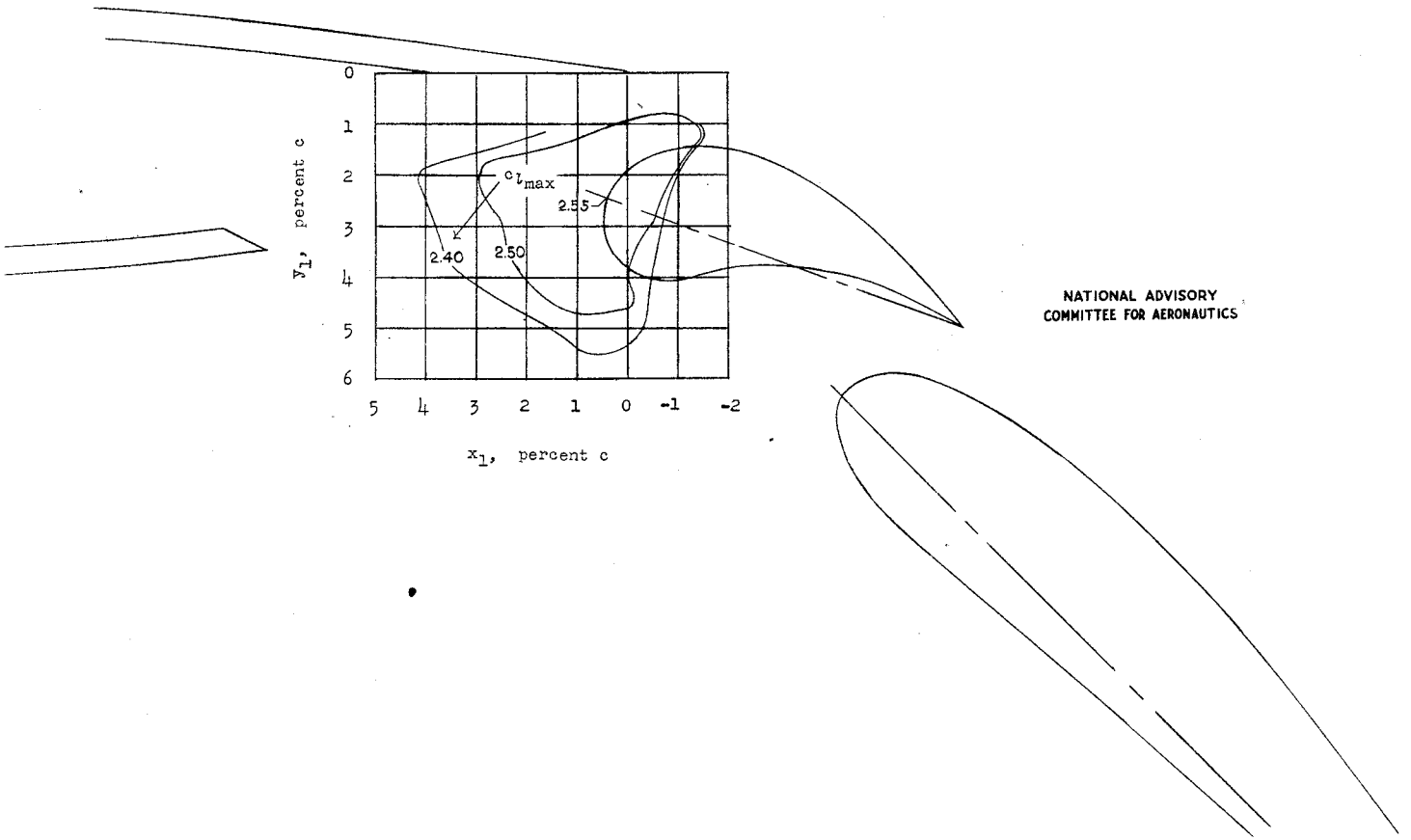

(b) $\delta_f = 45°$.

Figure 4.- Continued.

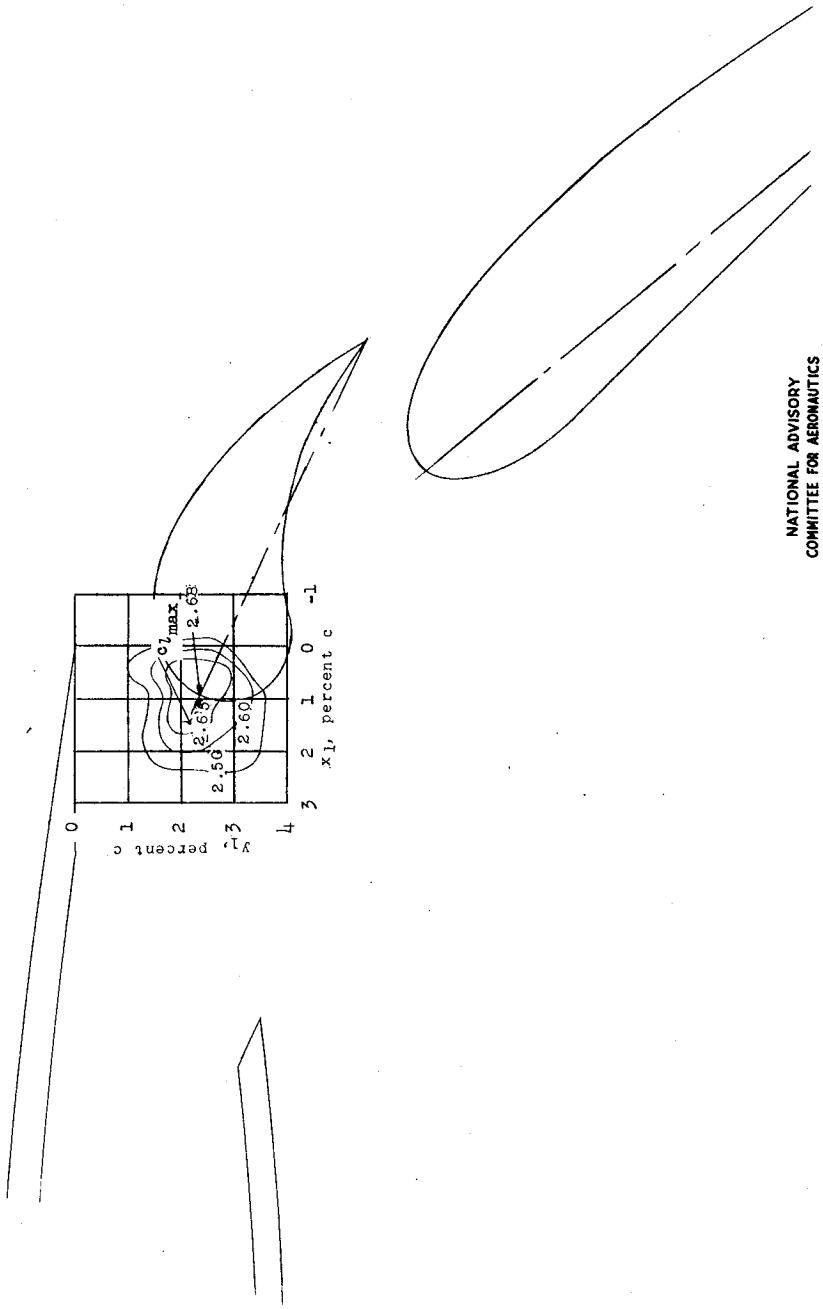

NATIONAL ADVISORY COMMITTEE FOR AERONAUTICS

(c) $\delta_f = 50°$.

Figure 4.- Continued.

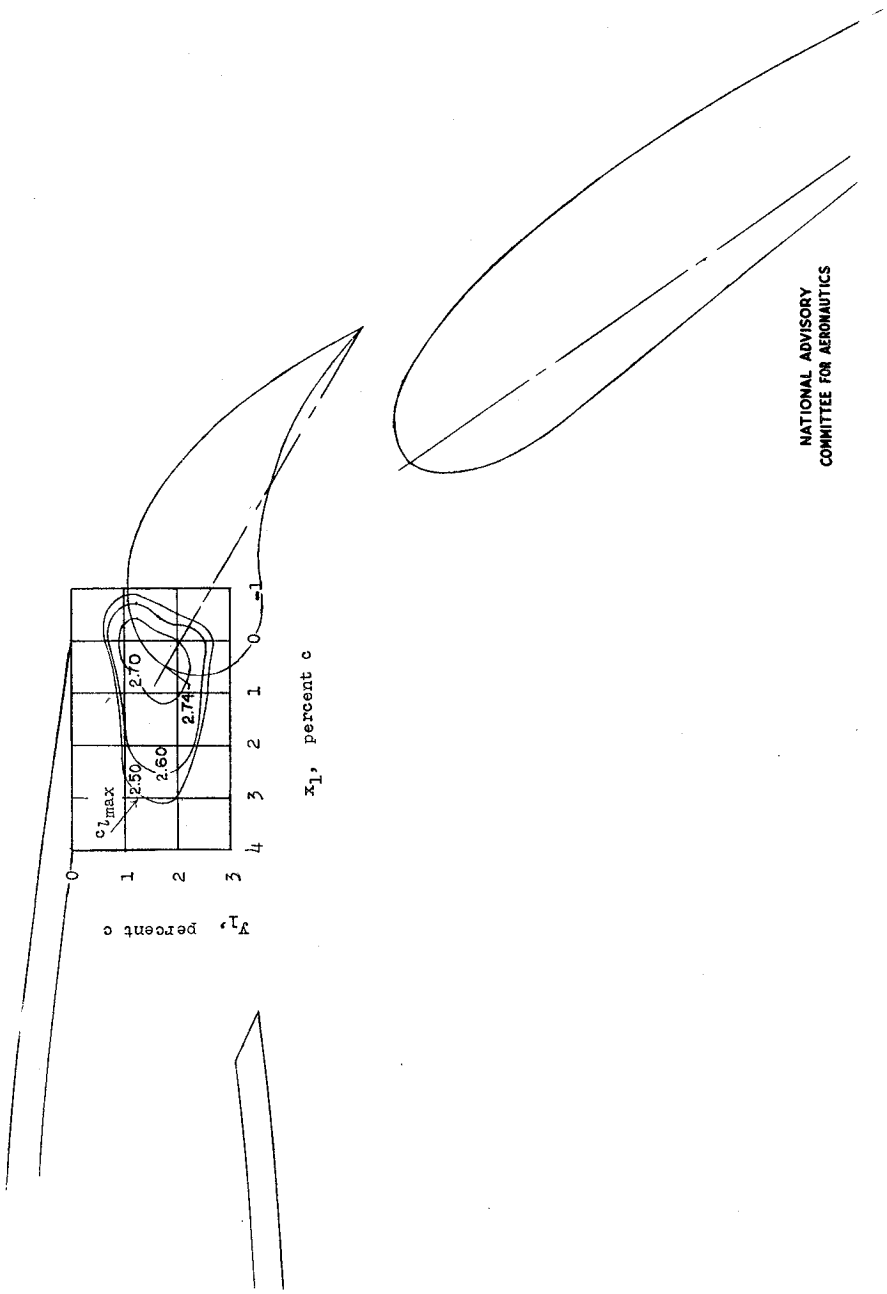

(d) $\delta_f = 55°$.

Figure 4.- Continued.

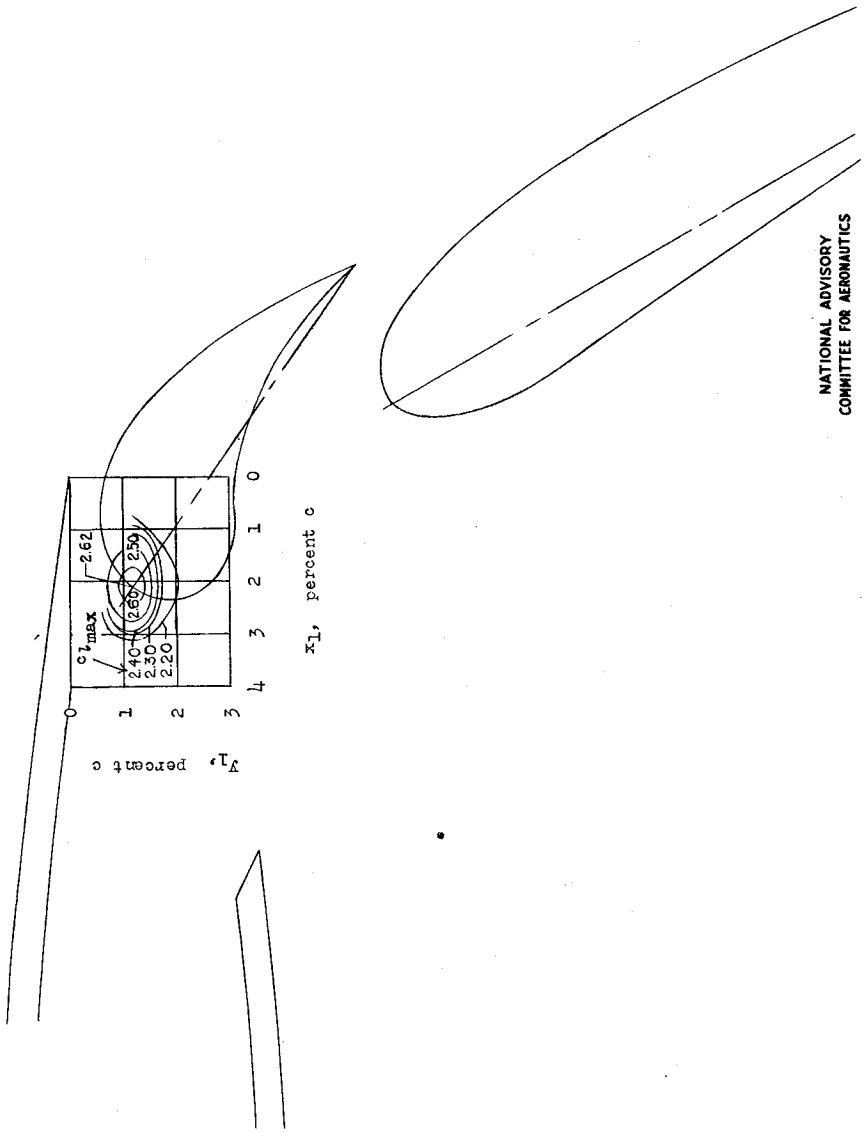

(e) $\delta_f = 60^\circ$.

Figure 4.- Concluded.

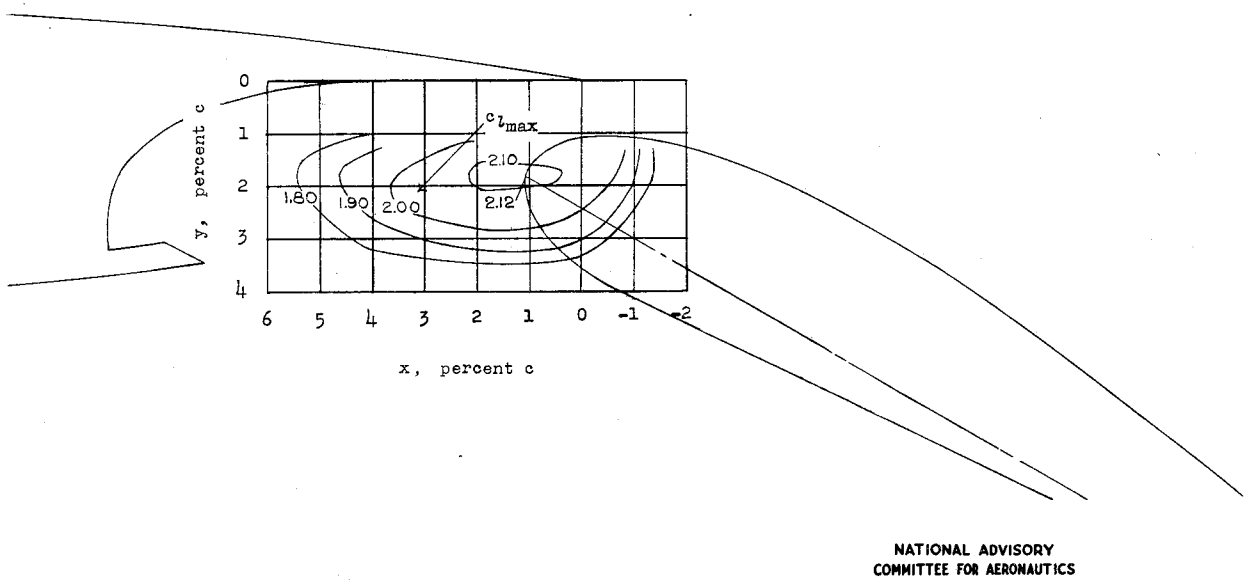

(a) $\delta_f = 30^\circ$.

Figure 5.- Contours of values of maximum lift coefficient for positions of slotted flap 1 at various flap deflections. NACA 65-210 airfoil; $R = 2.4 \times 10^6$ (approx.).

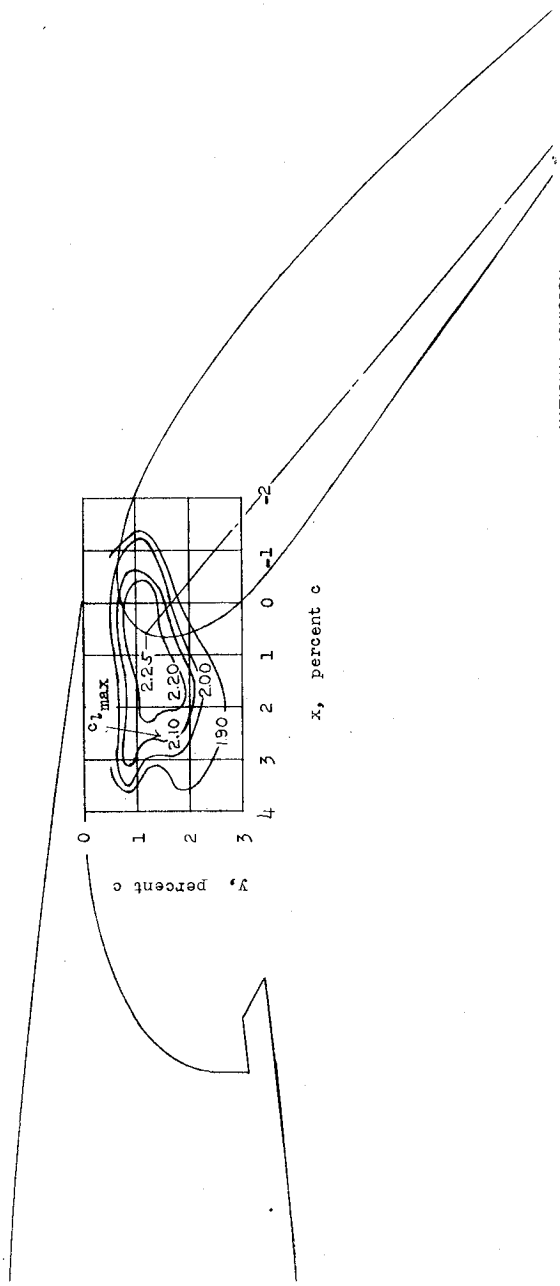

(b) $\delta_f = 40^\circ$.

Figure 5.- Continued.

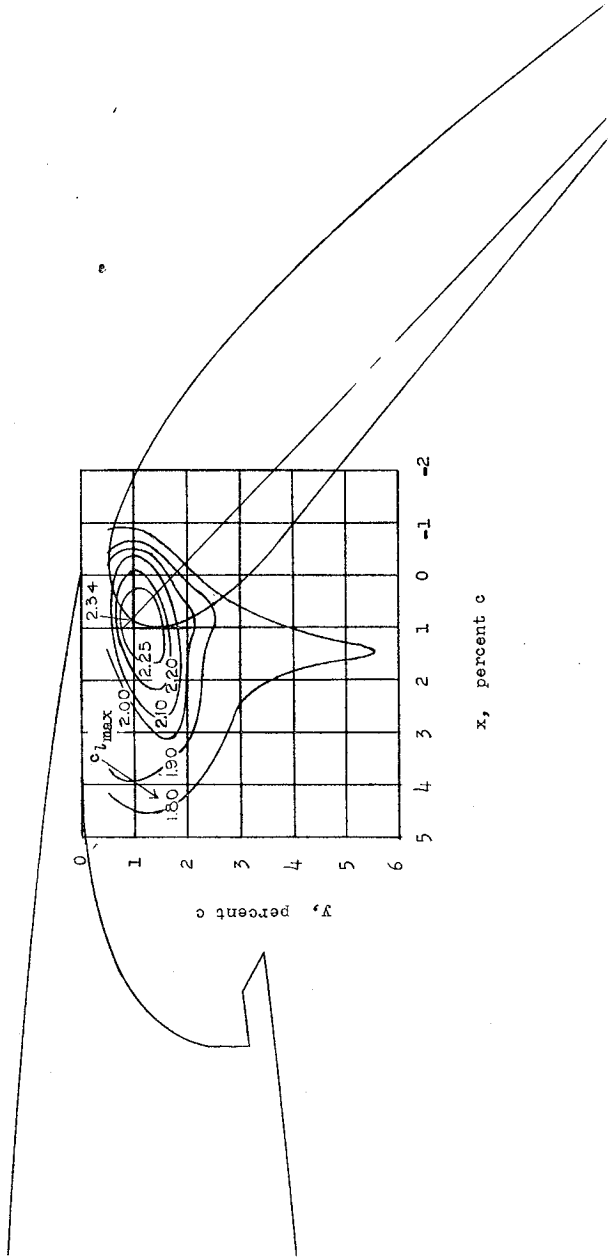

NATIONAL ADVISORY COMMITTEE FOR AERONAUTICS

(c) $\delta_f = 45°$.

Figure 5.- Continued.

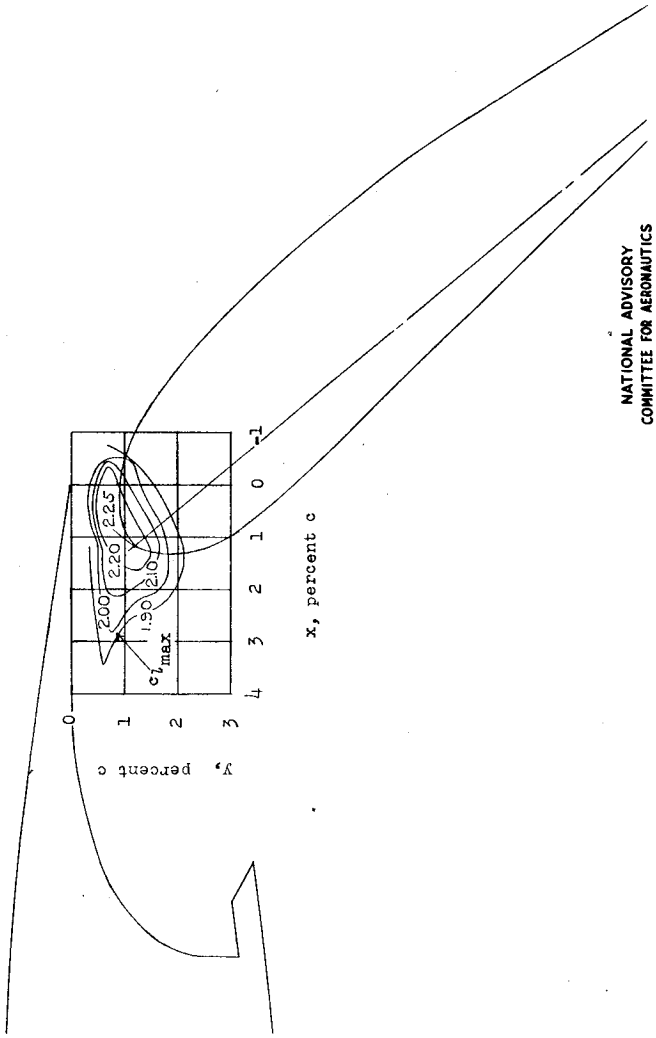

(d) $\delta_f = 50^\circ$.

Figure 5.- Concluded.

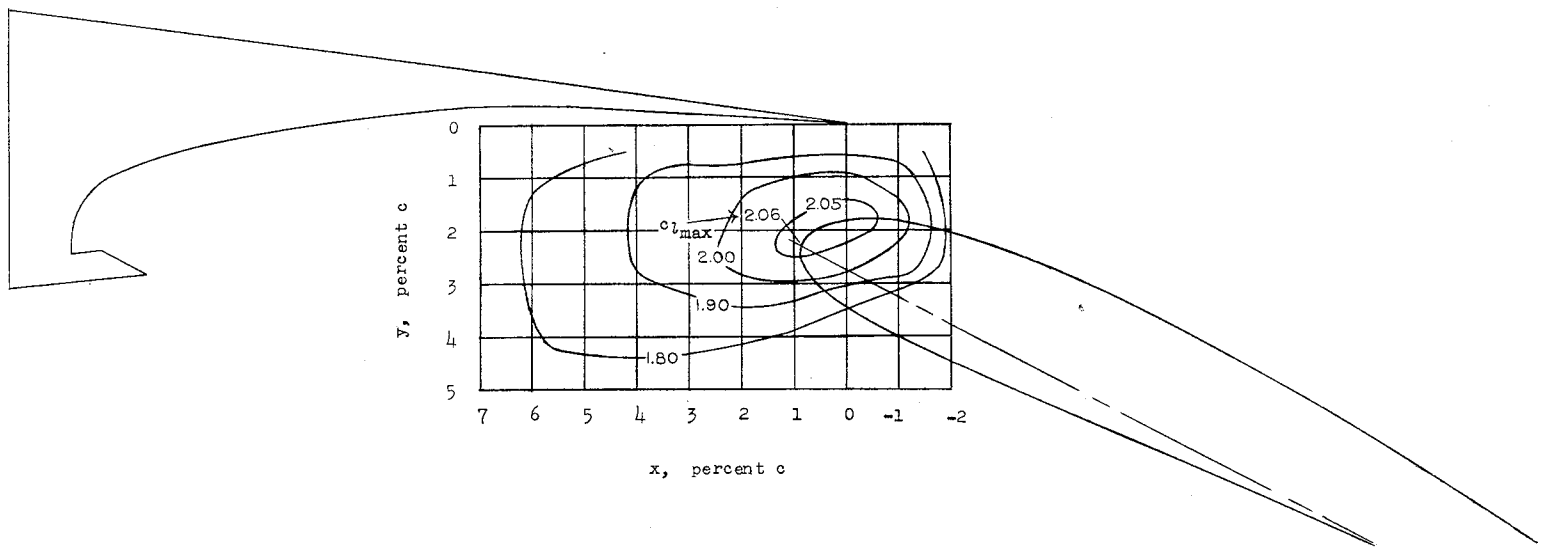

NATIONAL ADVISORY
COMMITTEE FOR AERONAUTICS

(a) $\delta_f = 30^\circ$.

Figure 6.- Contours of values of maximum lift coefficient for positions of slotted flap 2 at various flap deflections. NACA 65-210 airfoil; $R = 2.4 \times 10^6$ (approx.).

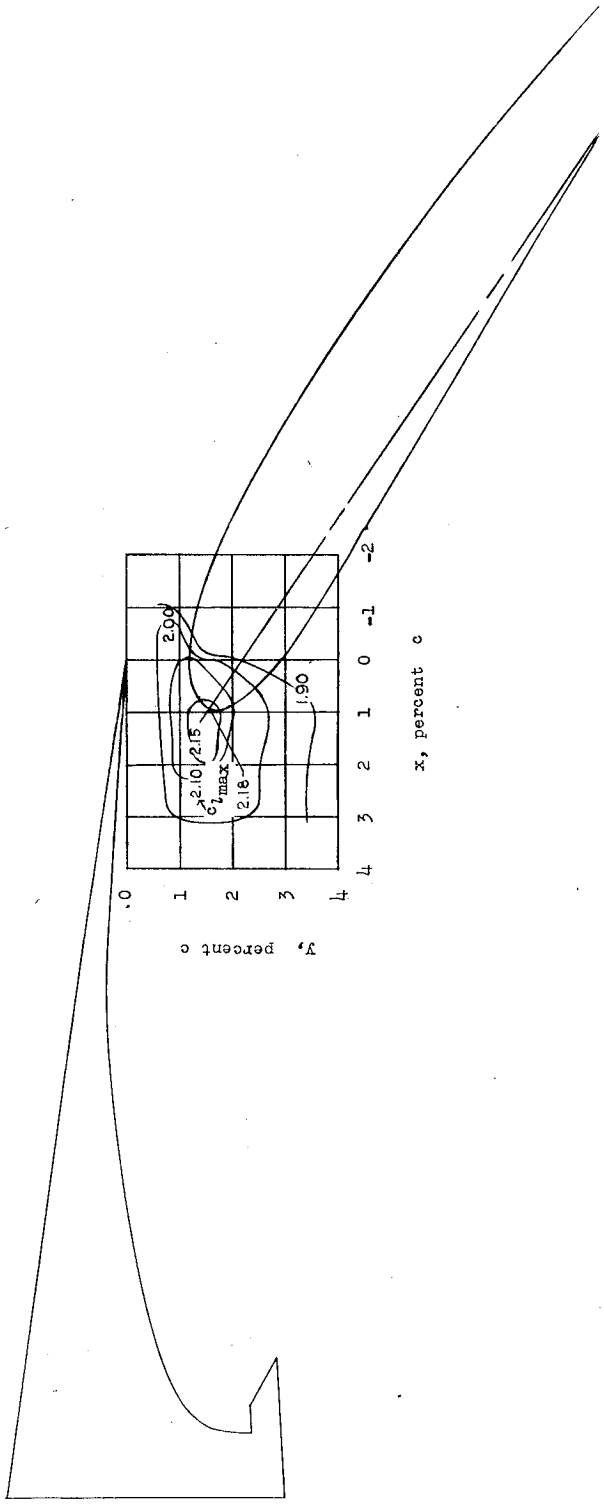

(b) $\delta_f = 36.3°$.

Figure 6.- Continued.

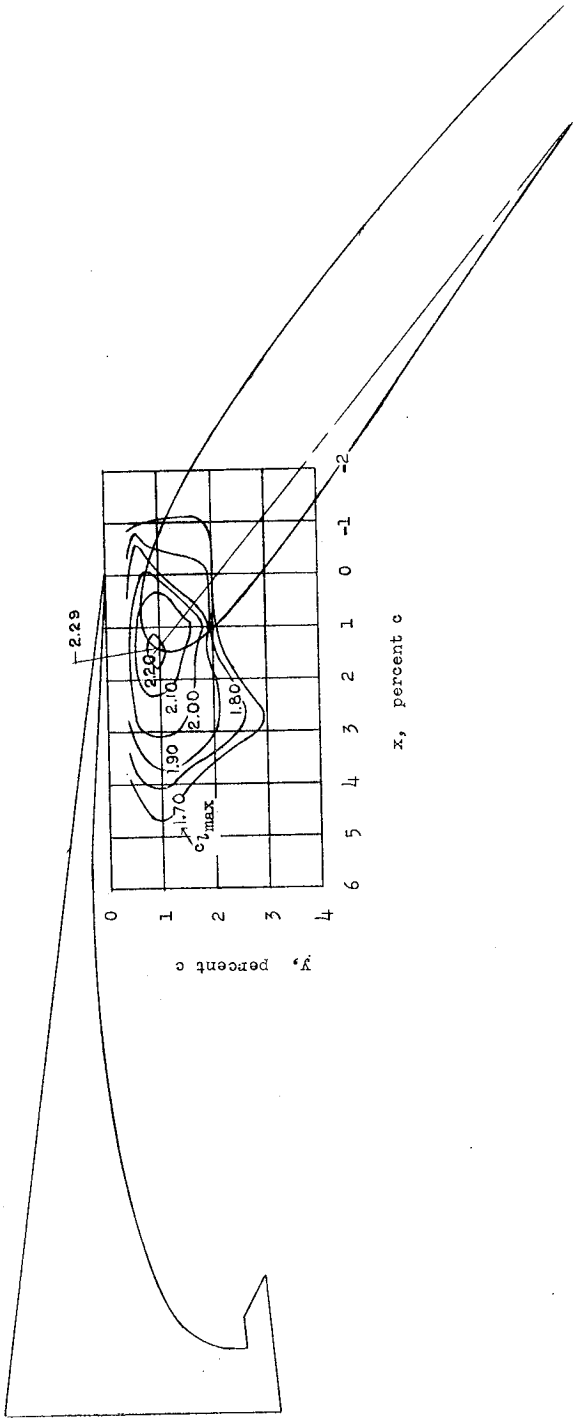

NATIONAL ADVISORY
COMMITTEE FOR AERONAUTICS

(c) $\delta_f = 41.3^\circ$.

Figure 6.- Continued.

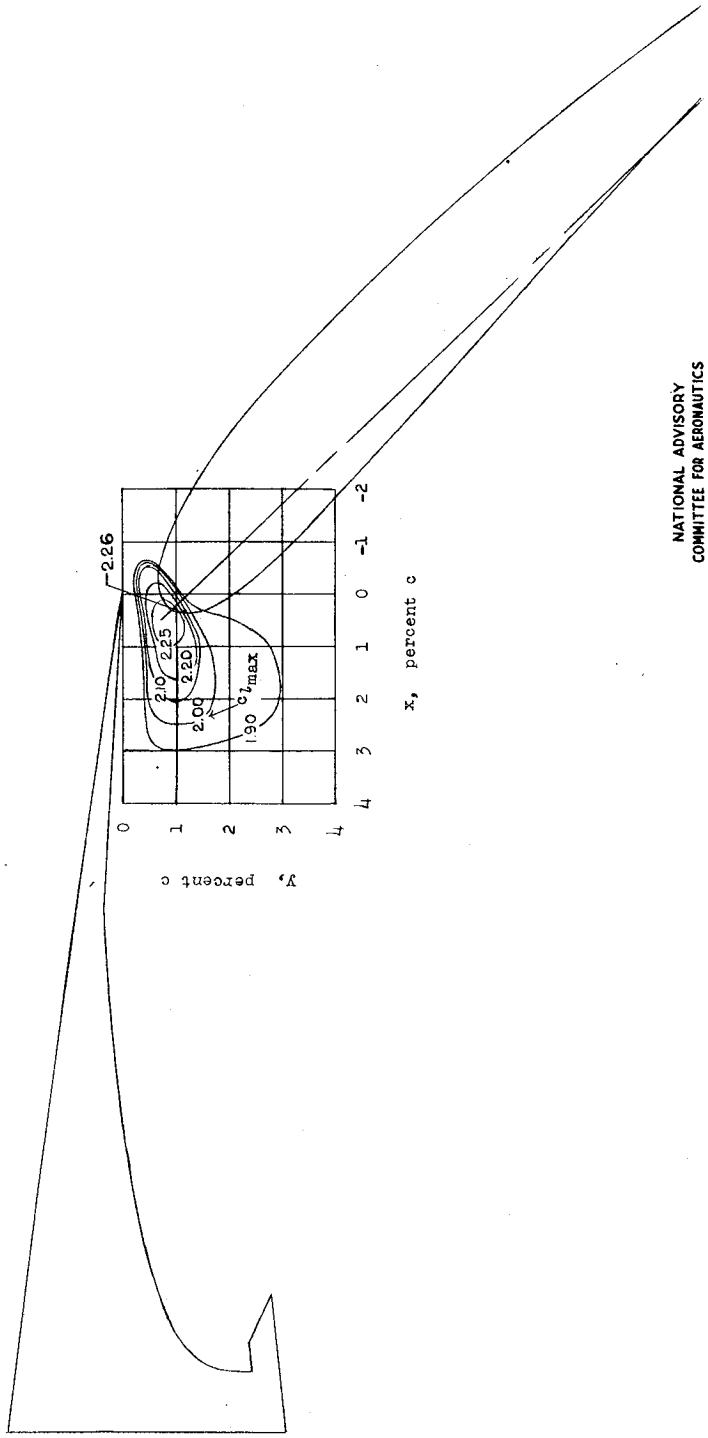

NATIONAL ADVISORY COMMITTEE FOR AERONAUTICS

(d) $\delta_f = 46.5°$.

Figure 6.- Concluded.

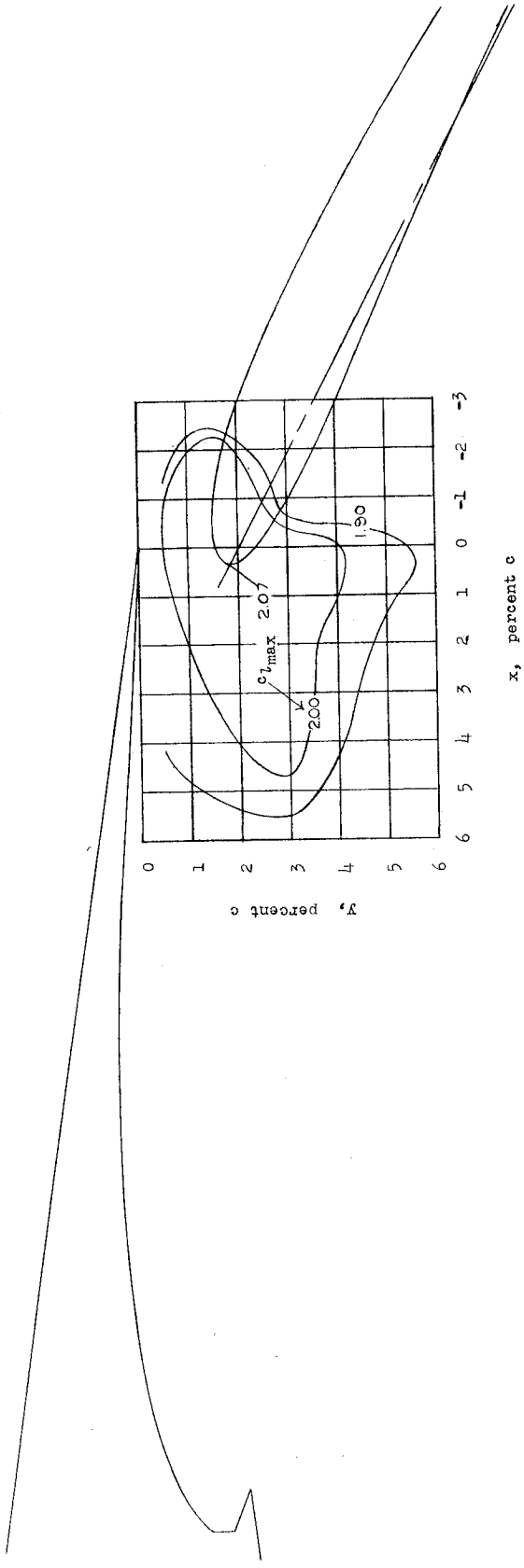

NATIONAL ADVISORY
COMMITTEE FOR AERONAUTICS

(a) $\delta_f = 30°$.

Figure 7.- Contours of values of maximum lift coefficient for positions of slotted flap 3 at various flap deflections. NACA 65-210 airfoil; $R = 2.4 \times 10^6$ (approx.).

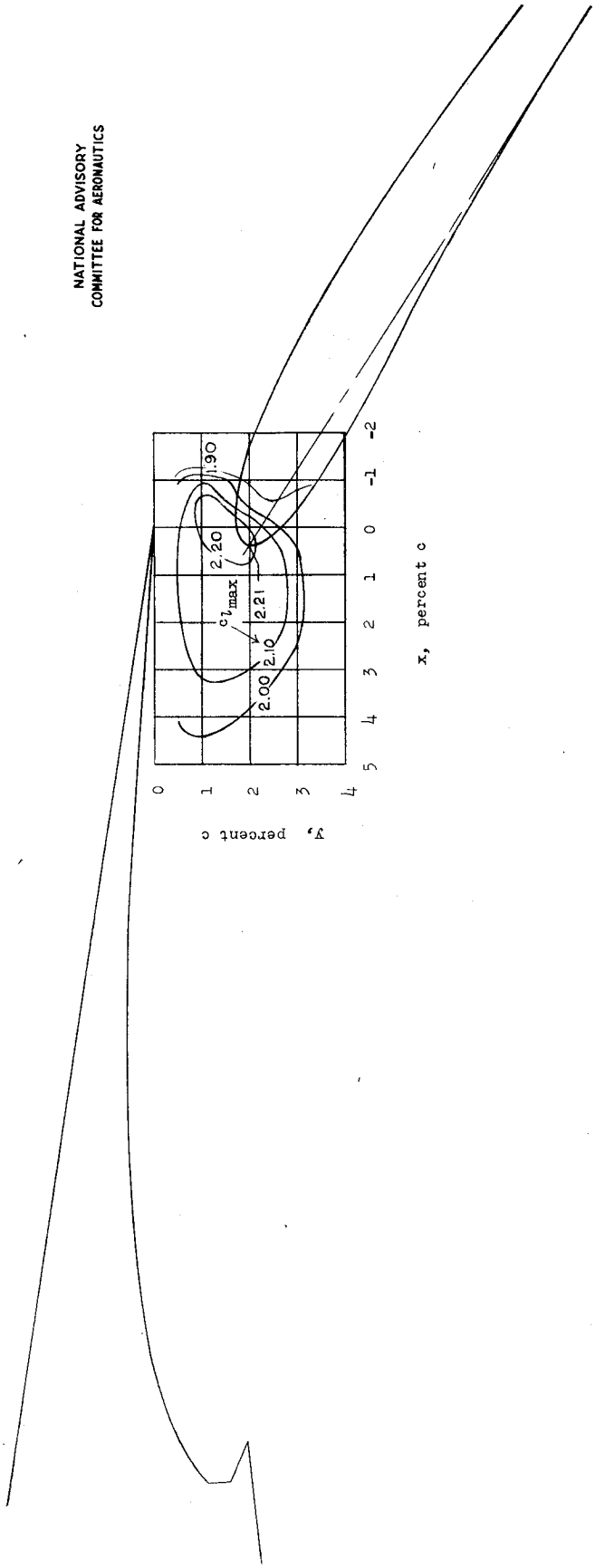

(b) $\delta_f = 35°$.

Figure 7.- Continued.

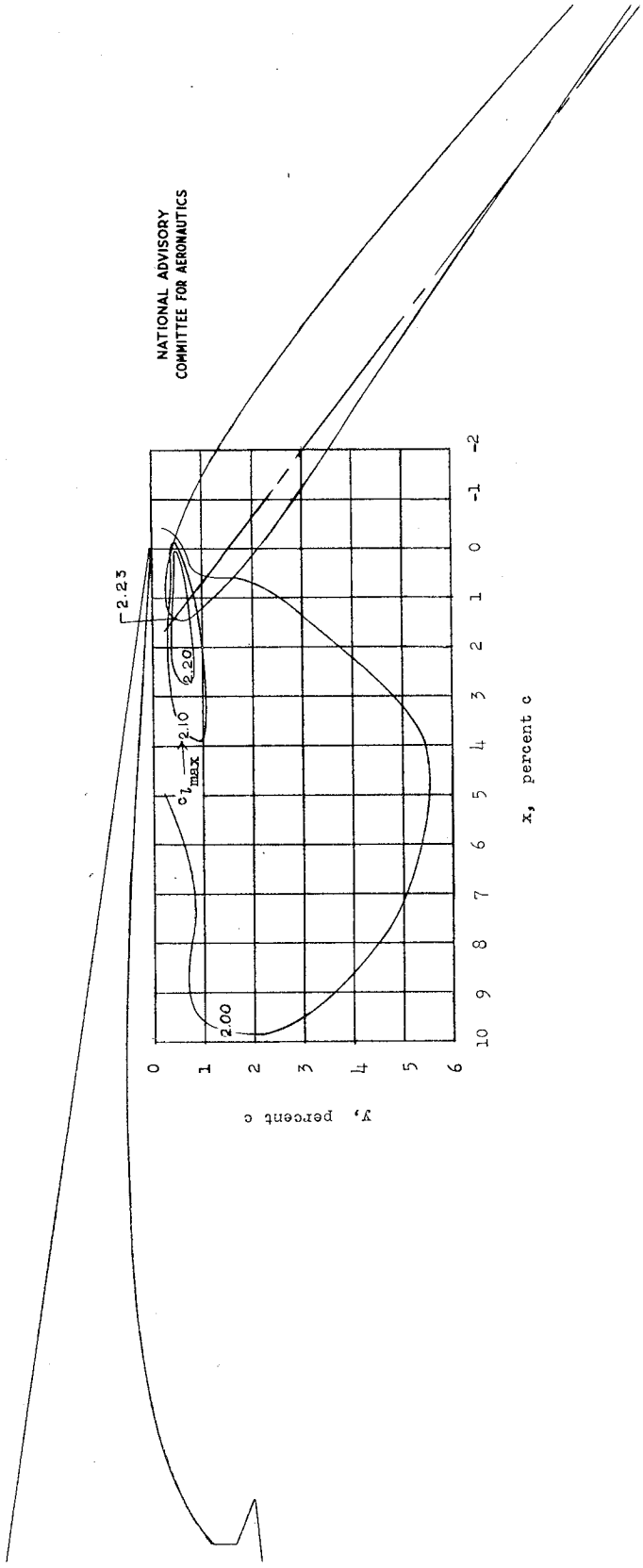

(c) $\delta_f = 40°$.

Figure 7.- Concluded.

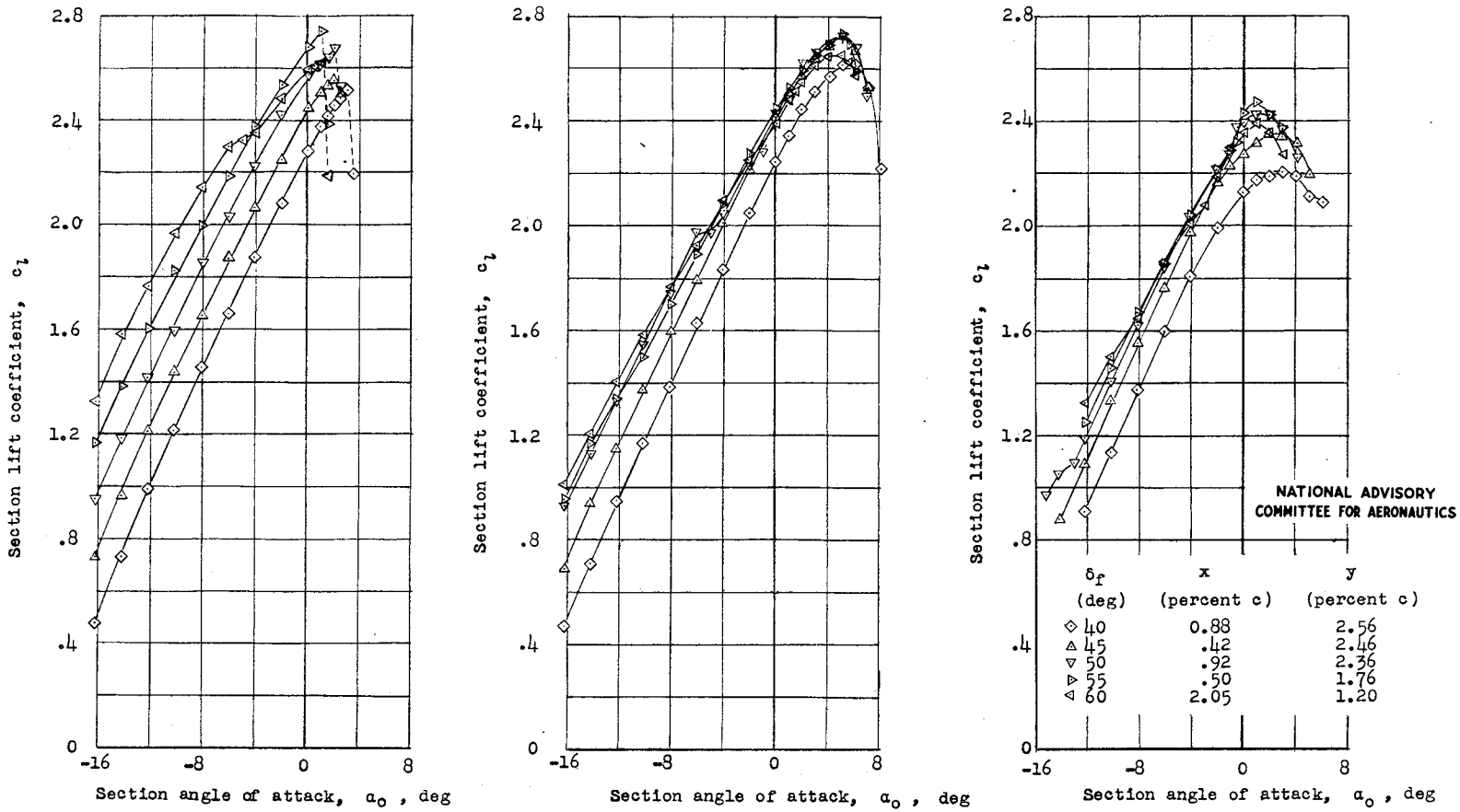

(a) $R = 2.4 \times 10^6$ (approx.); smooth. (b) $R = 6.0 \times 10^6$ (approx.); smooth. (c) $R = 6.0 \times 10^6$ (approx.); standard L.E. roughness.

Figure 8.- Section lift characteristics of the NACA 65-210 airfoil with a 0.312c double slotted flap.

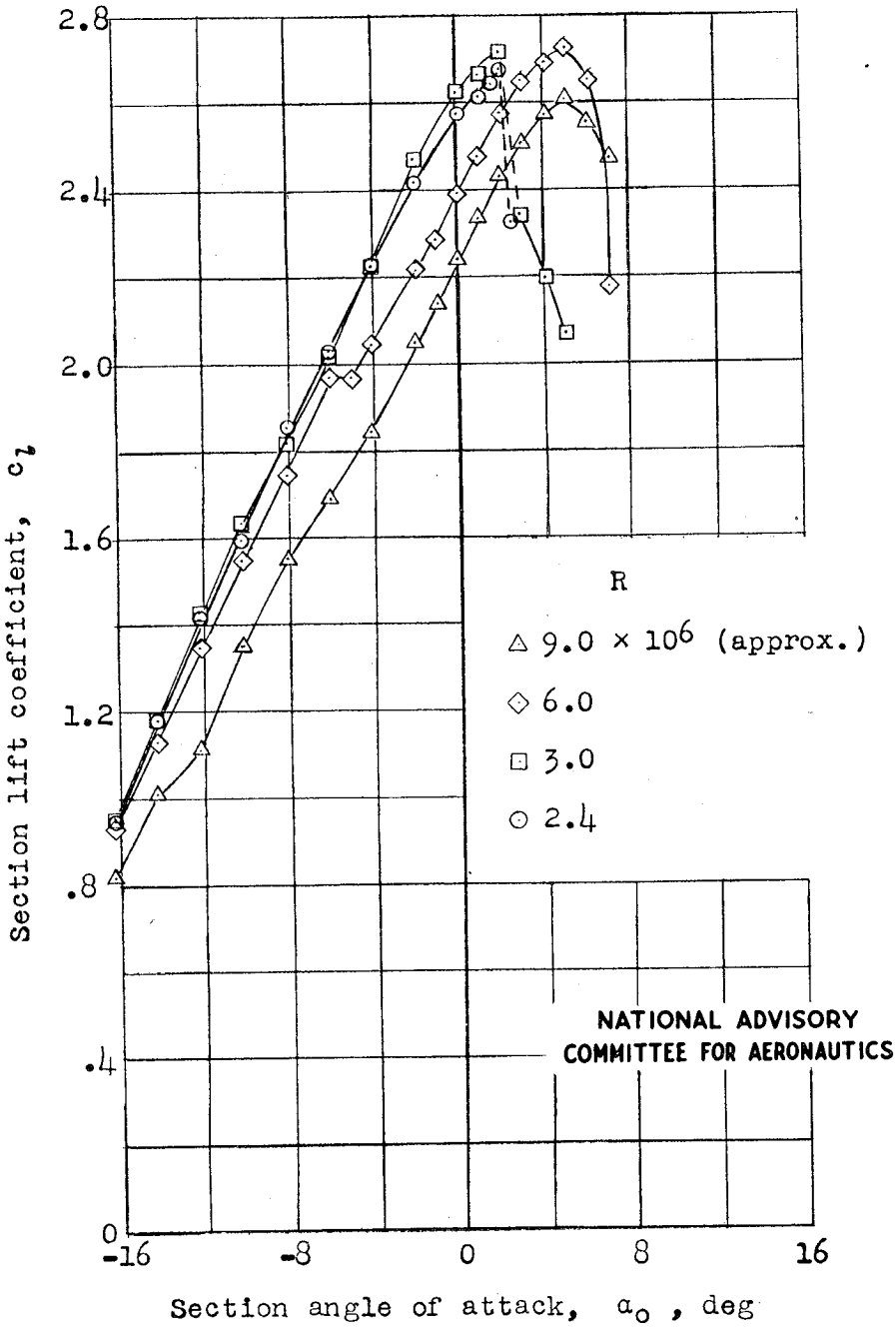

Figure 9.- Section lift characteristics of the NACA 65-210 airfoil with a 0.312c double slotted flap at various Reynolds numbers. $\delta_f = 50^o$; x = 0.92; y = 2.36.

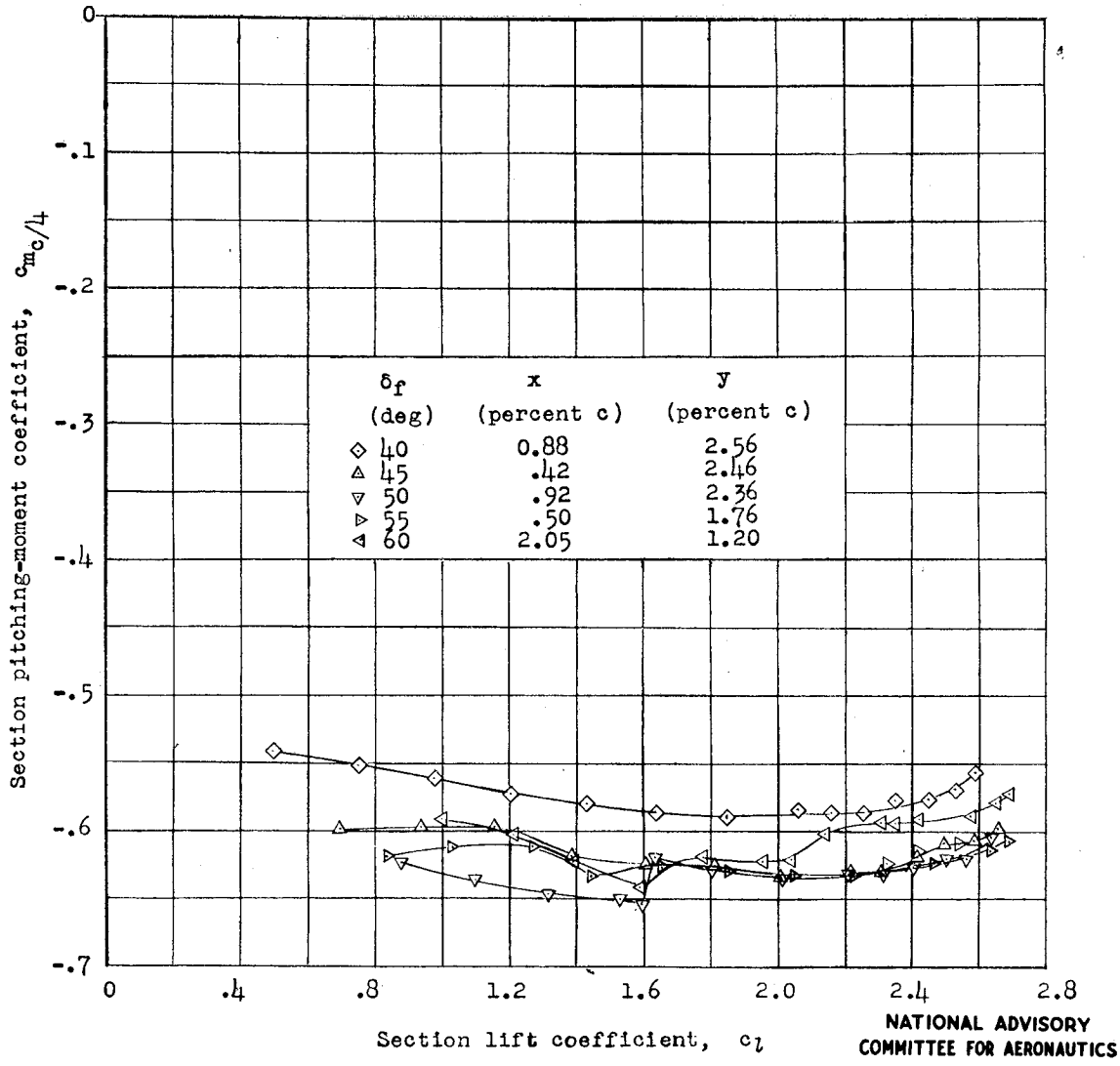

Figure 10.- Section pitching-moment characteristics of the NACA 65-210 airfoil with a 0.312c double slotted flap. $R = 6.0 \times 10^6$ (approx.).

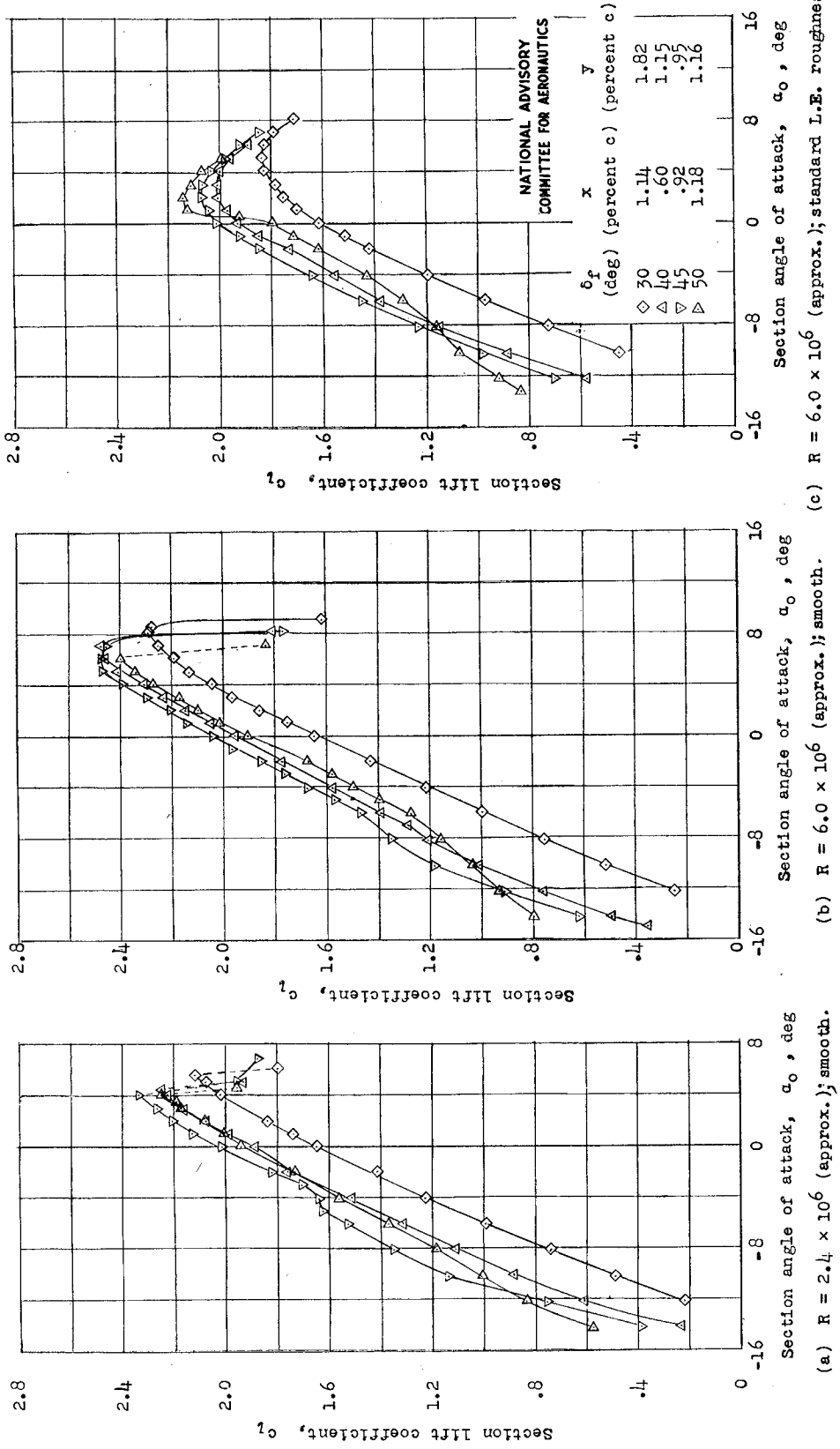

Figure 11.- Section lift characteristics of the NACA 65-210 airfoil with slotted flap 1.

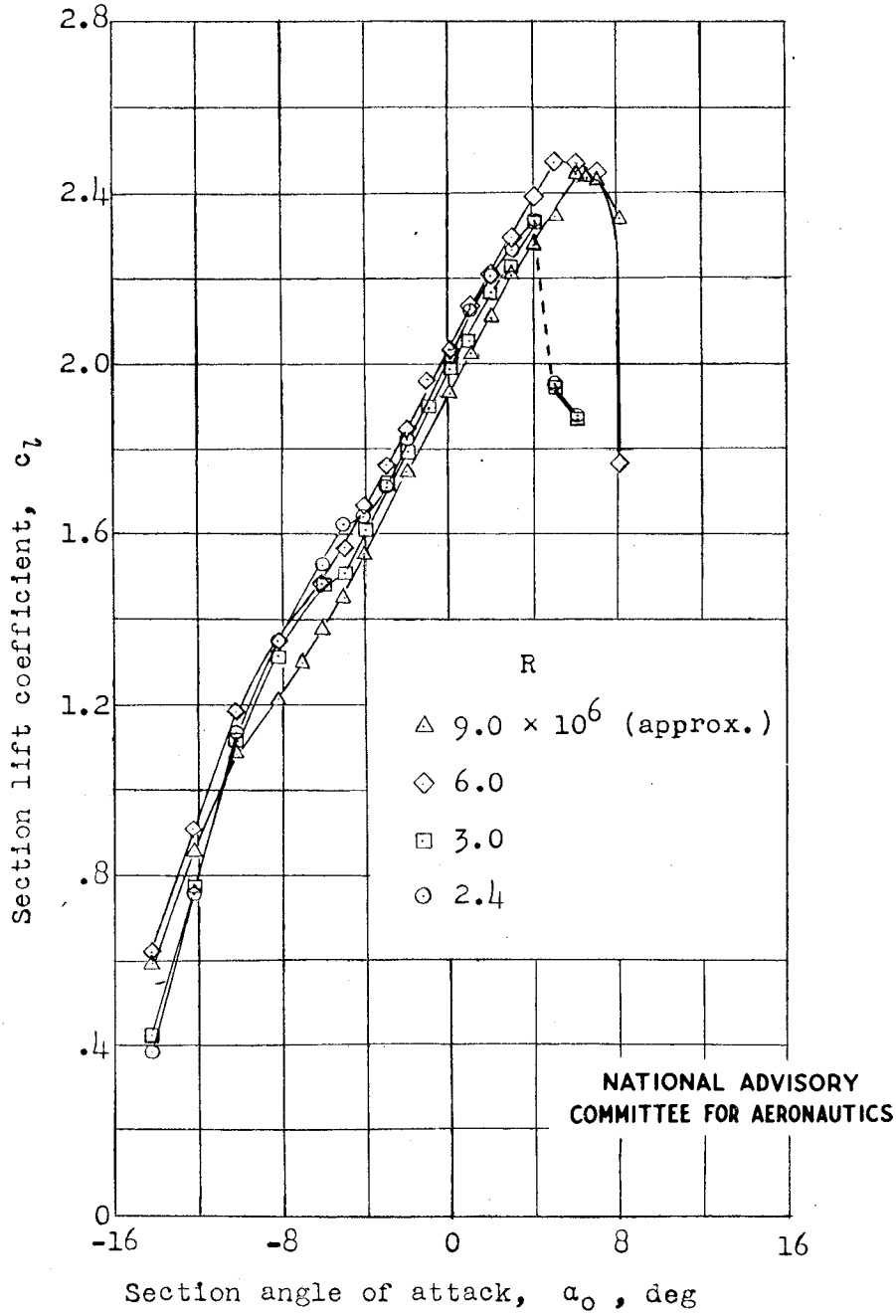

Figure 12.- Section lift characteristics of the NACA 65-210 airfoil with slotted flap 1 at various Reynolds numbers. $\delta_f = 45^\circ$; $x = 0.92$; $y = 0.95$.

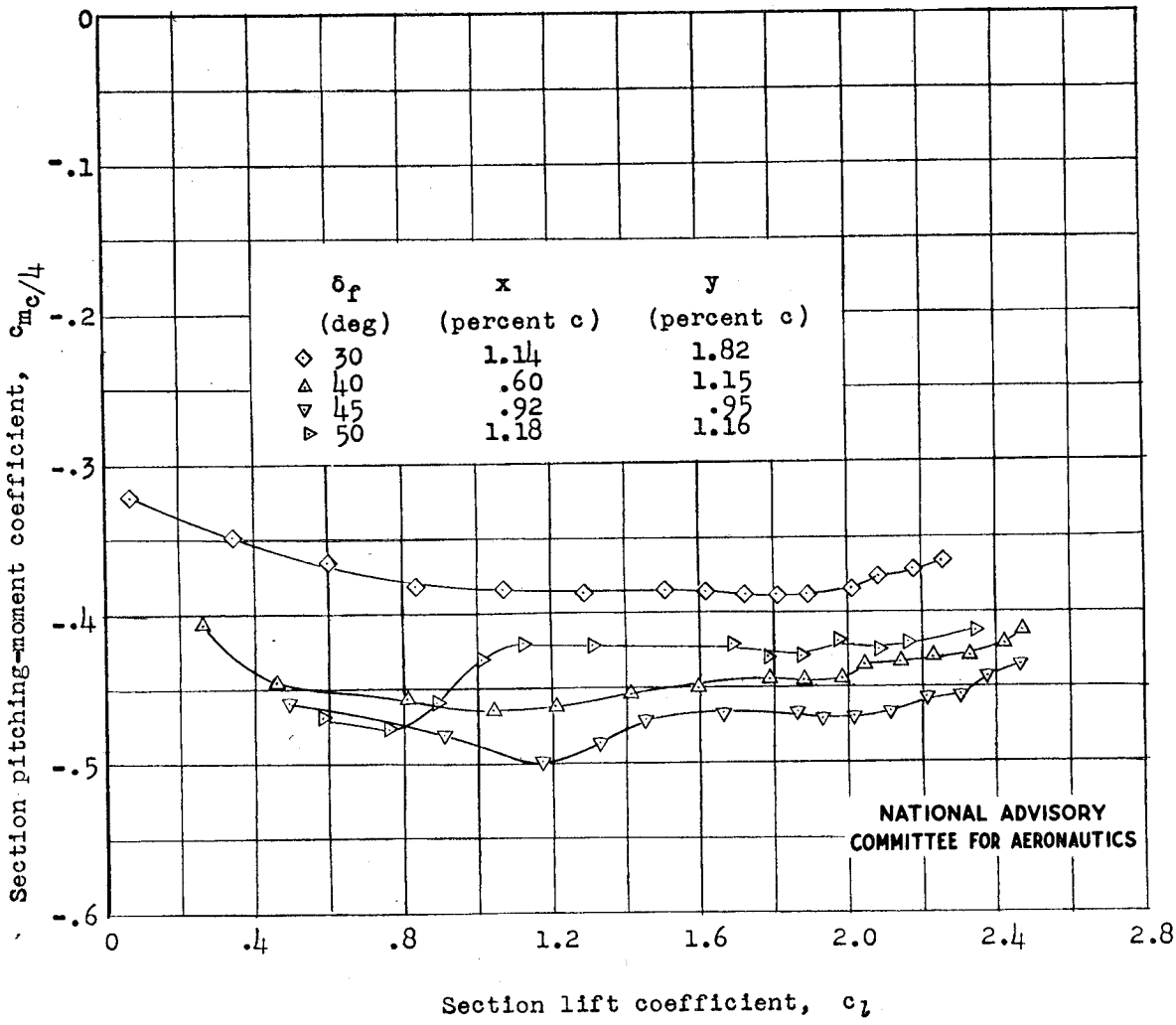

Figure 13.- Section pitching-moment characteristics of the NACA 65-210 airfoil with slotted flap 1. $R = 6.0 \times 10^6$ (approx.).

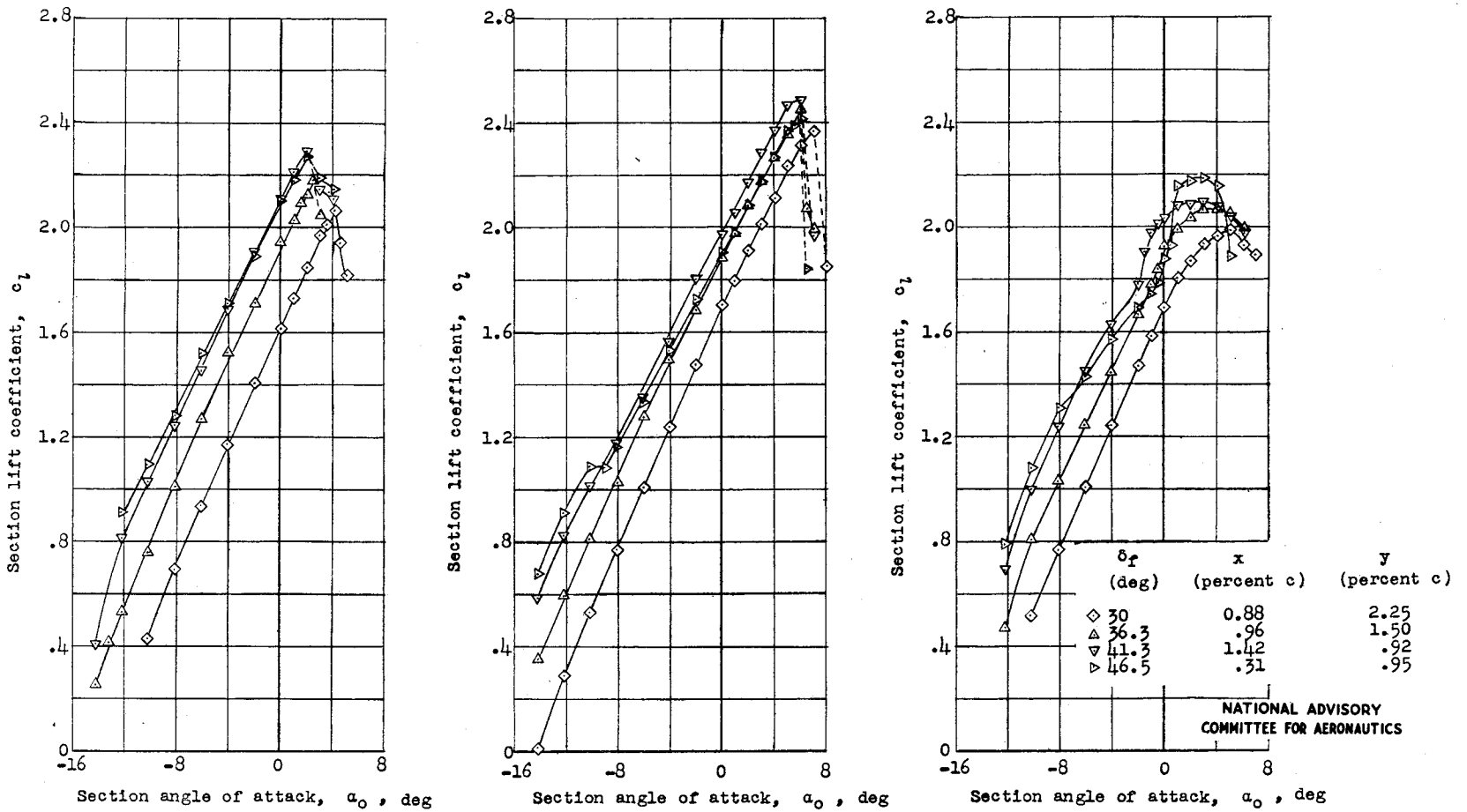

(a) R = 2.4×10^6 (approx.); smooth. (b) R = 6.0×10^6 (approx.); smooth. (c) R = 6.0×10^6 (approx.); standard L.E. roughness.

Figure 14.- Section lift characteristics of the NACA 65-210 airfoil with slotted flap 2.

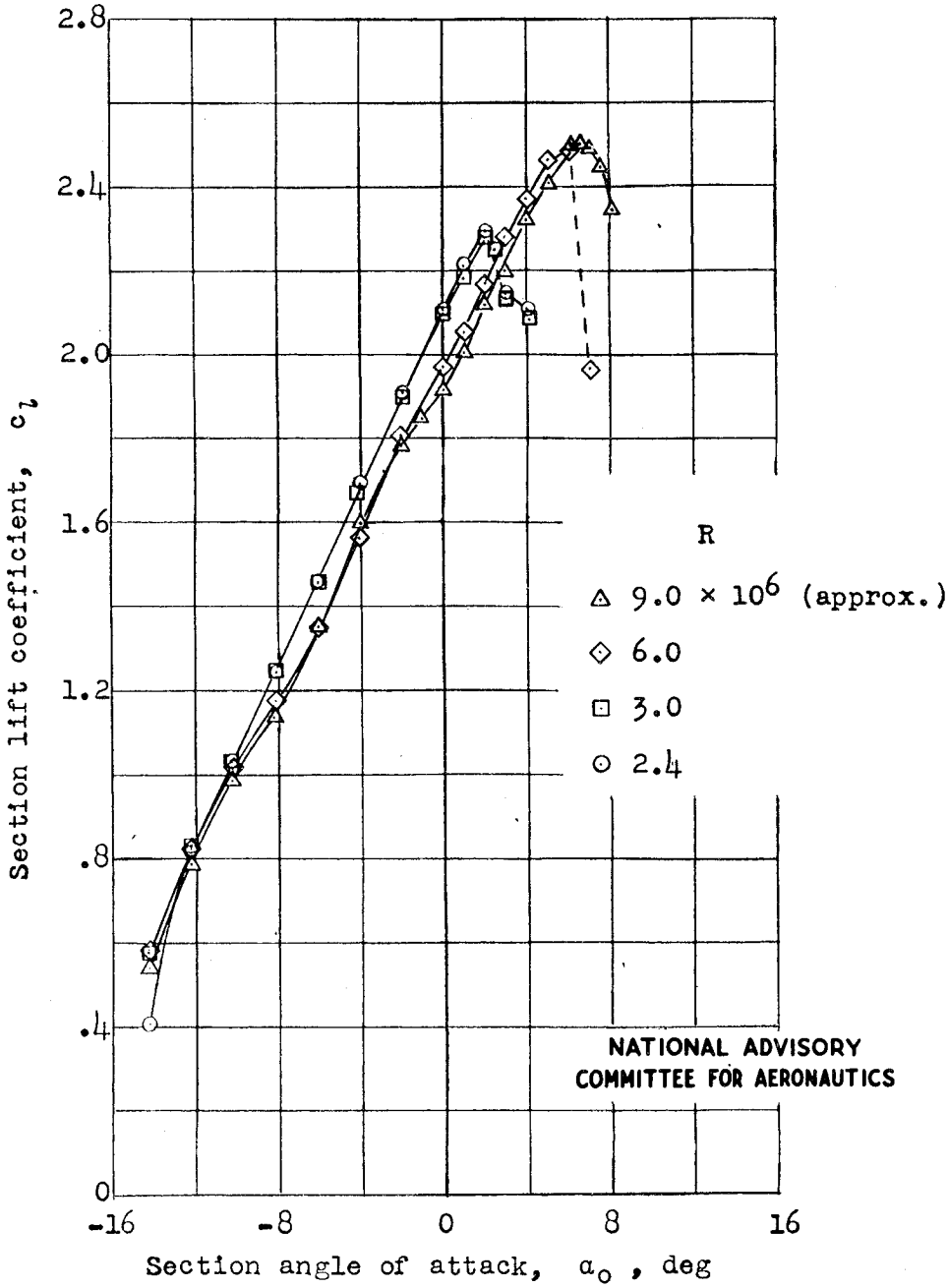

Figure 15.- Section lift characteristics of the NACA 65-210 airfoil with slotted flap 2 at various Reynolds numbers. $\delta_f = 41.3^\circ$; $x = 1.42$; $y = 0.92$.

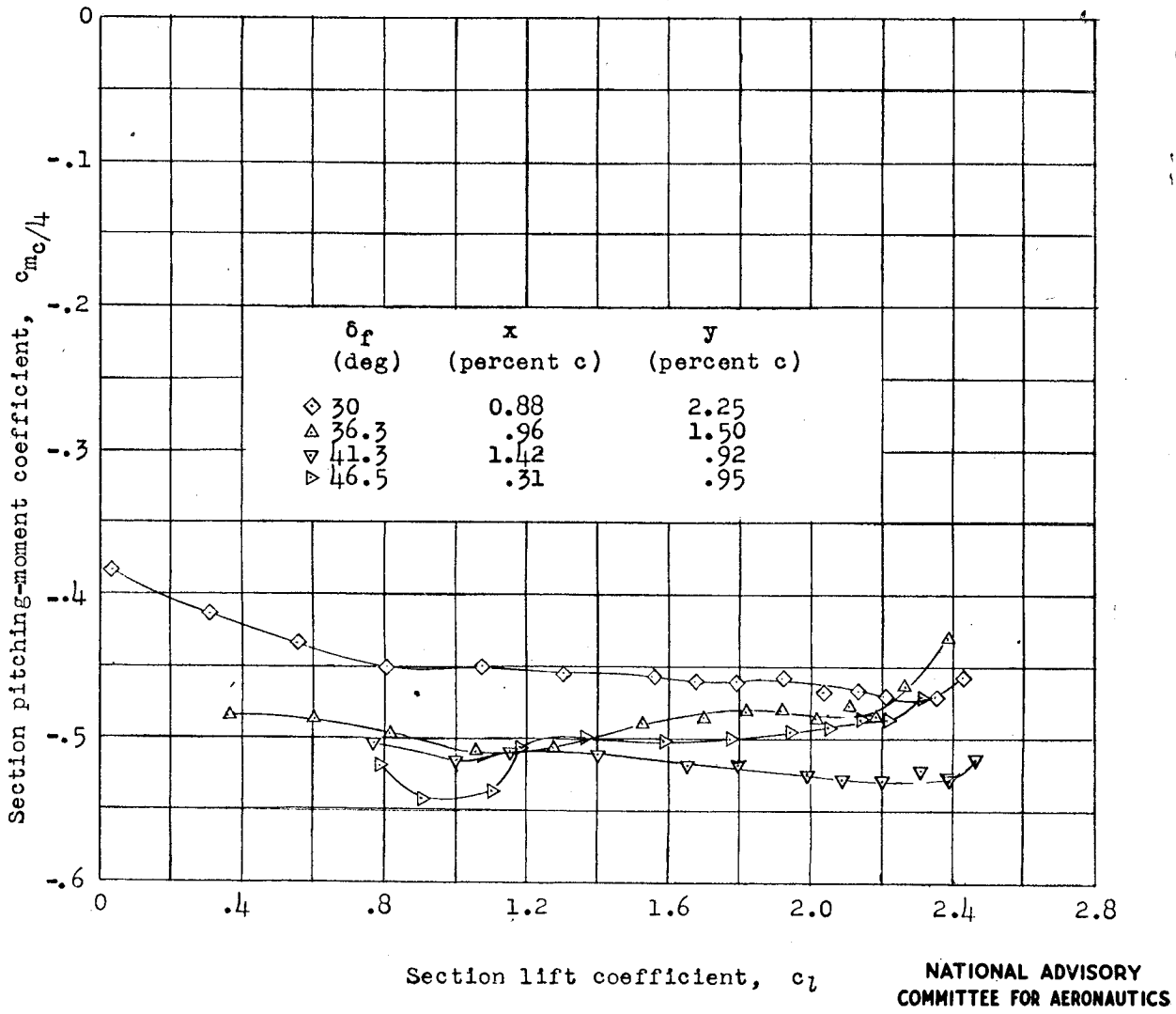

Figure 16.- Section pitching-moment characteristics of the NACA 65-210 airfoil with slotted flap 2. $R = 6.0 \times 10^6$ (approx.).

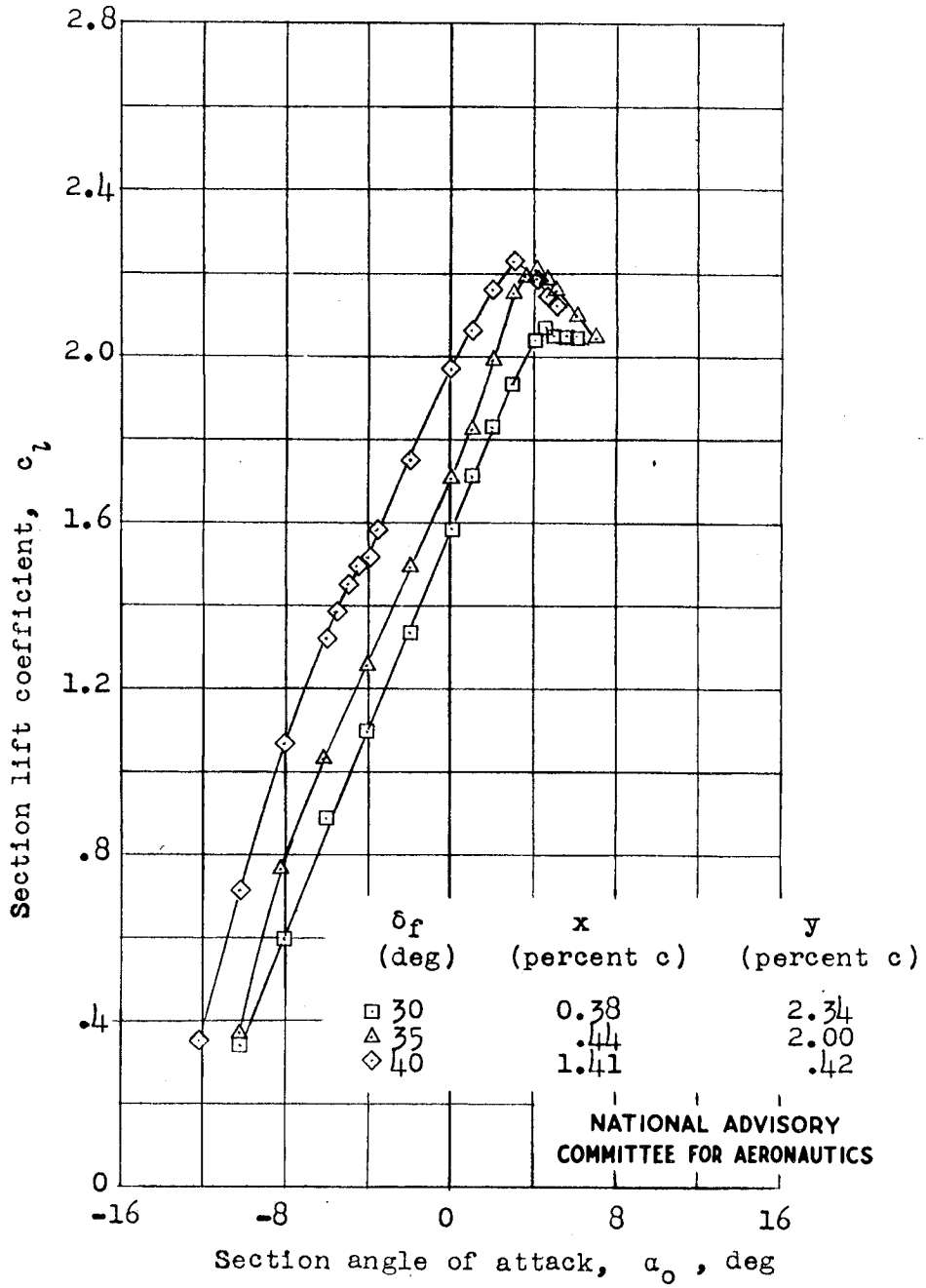

Figure 17.- Section lift characteristics of the NACA 65-210 airfoil with slotted flap 3. $R = 2.4 \times 10^6$ (approx.); smooth.

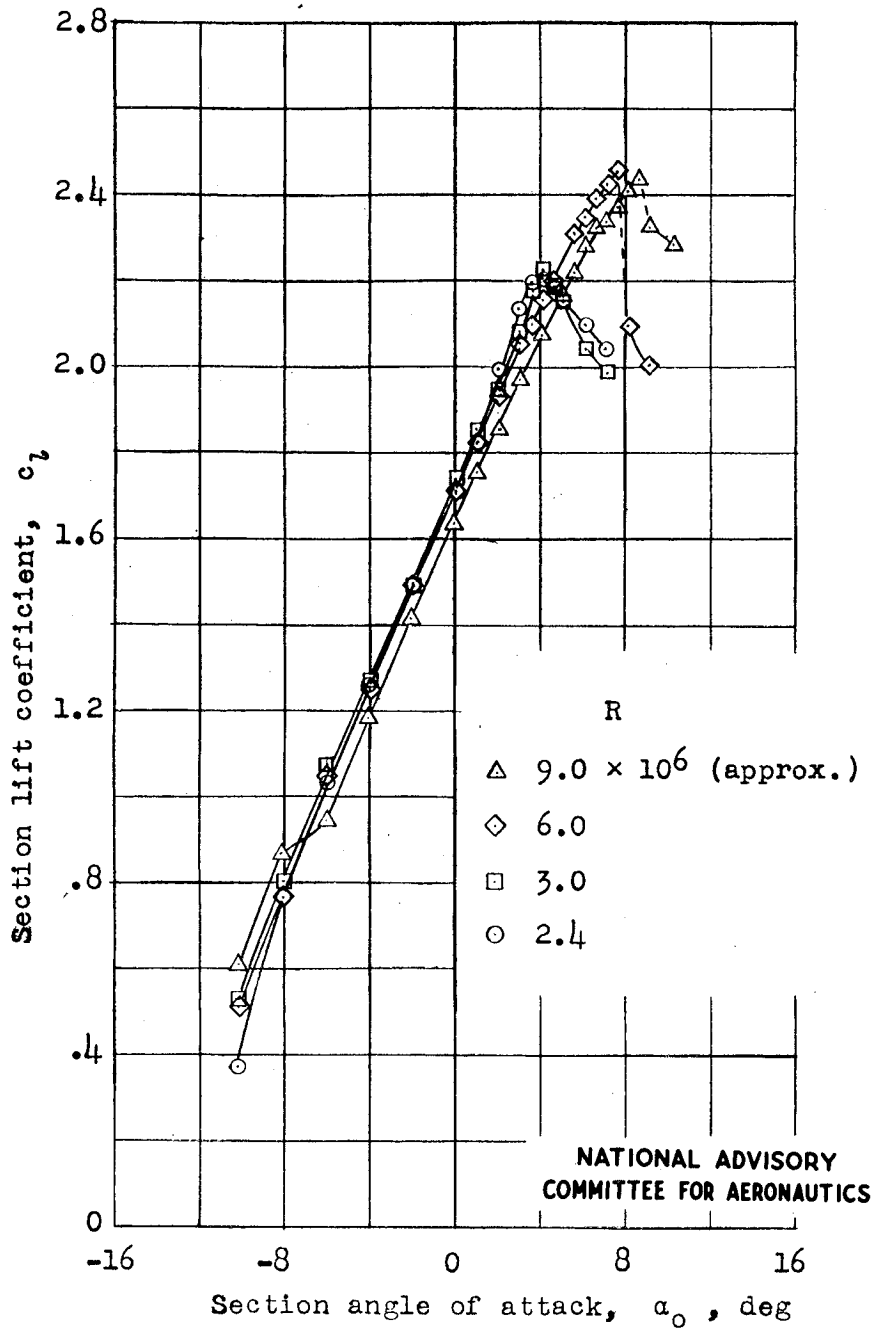

Figure 18.- Section lift characteristics of the NACA 65-210 airfoil with slotted flap 3 at various Reynolds numbers. $\delta_f = 35^o$; $x = 0.44$; $y = 2.00$.

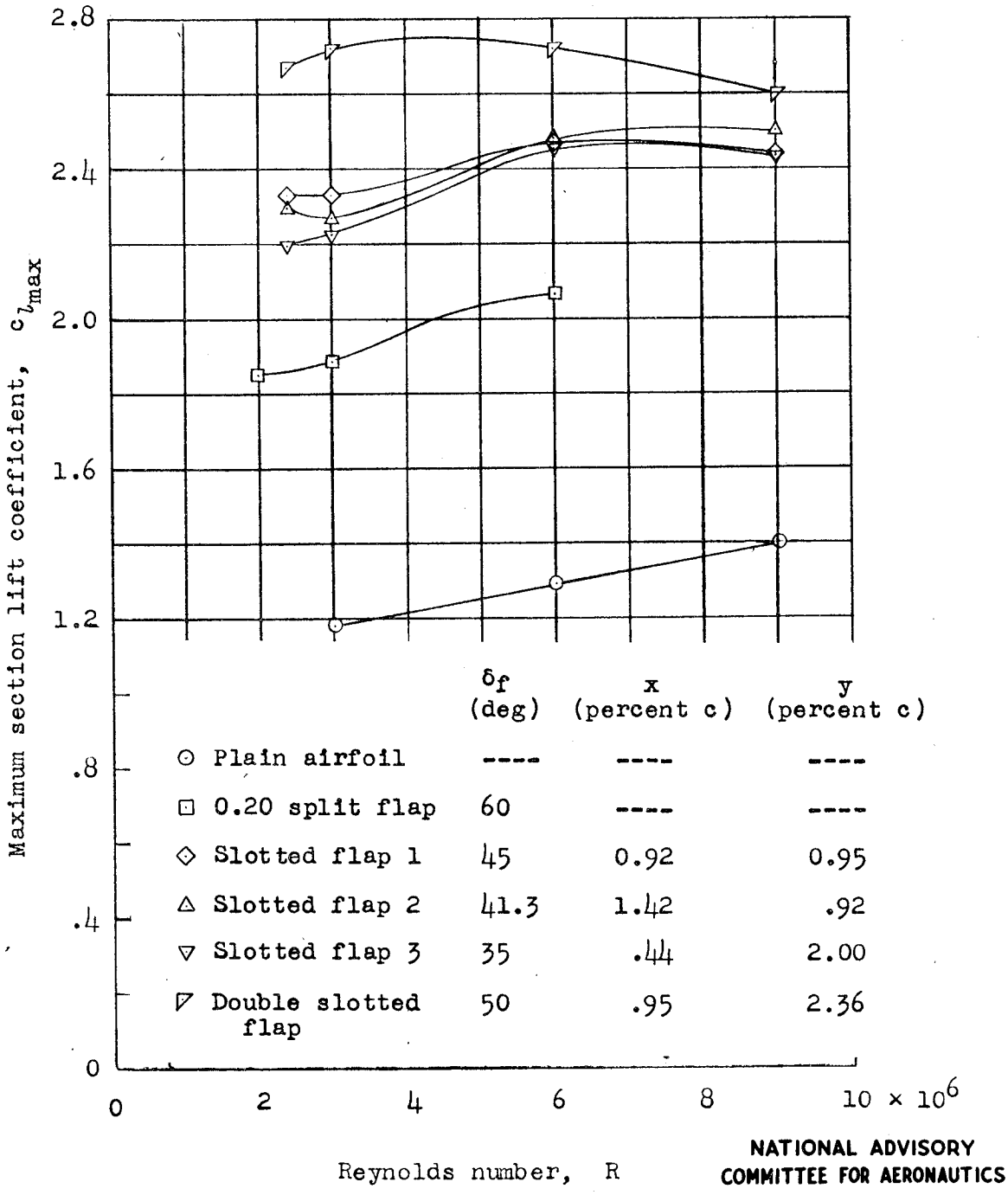

Figure 19.- Variation of maximum section lift coefficient with Reynolds number for various types of flap on the NACA 65-210 airfoil section.

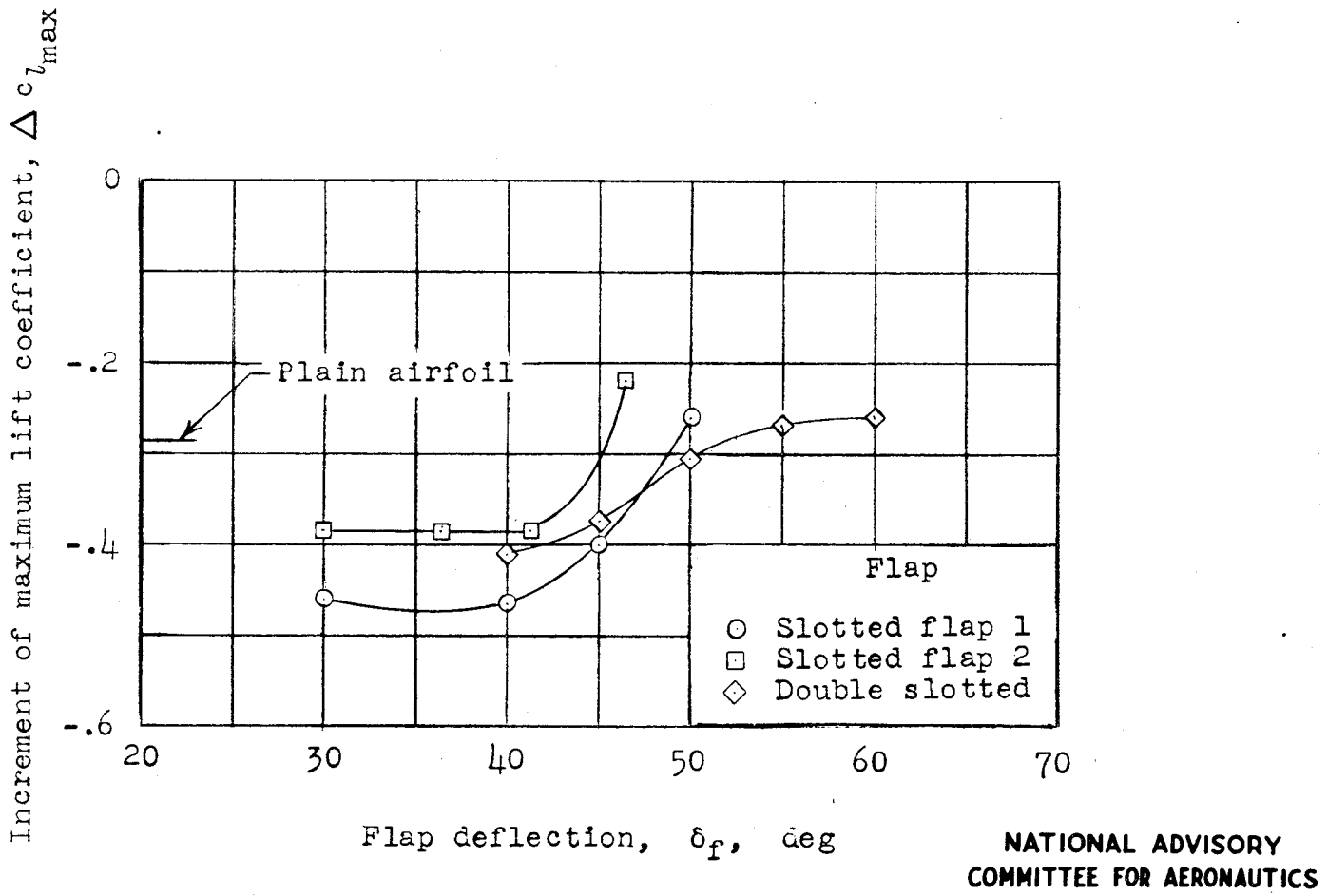

Figure 20.- Effect of roughness on maximum lifts of the NACA 65-210 airfoil section with various types of flap. $R = 6.0 \times 10^6$ (approx.).

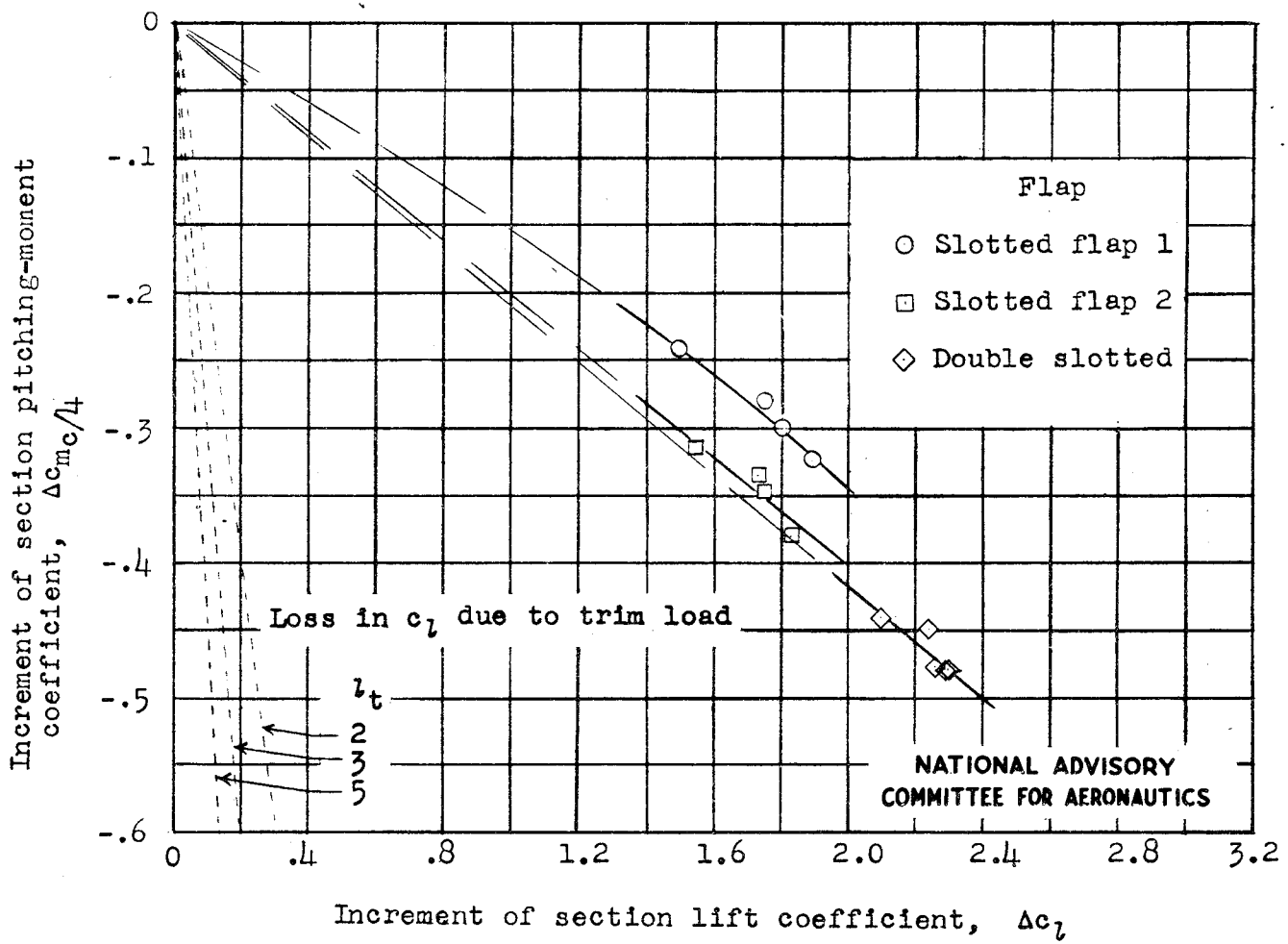

Figure 21.- Variation of increment of pitching-moment coefficient with increment of lift coefficient at constant angle of attack caused by deflection of various flaps on the 65-210 airfoil section. $\alpha_o = 0^\circ$.

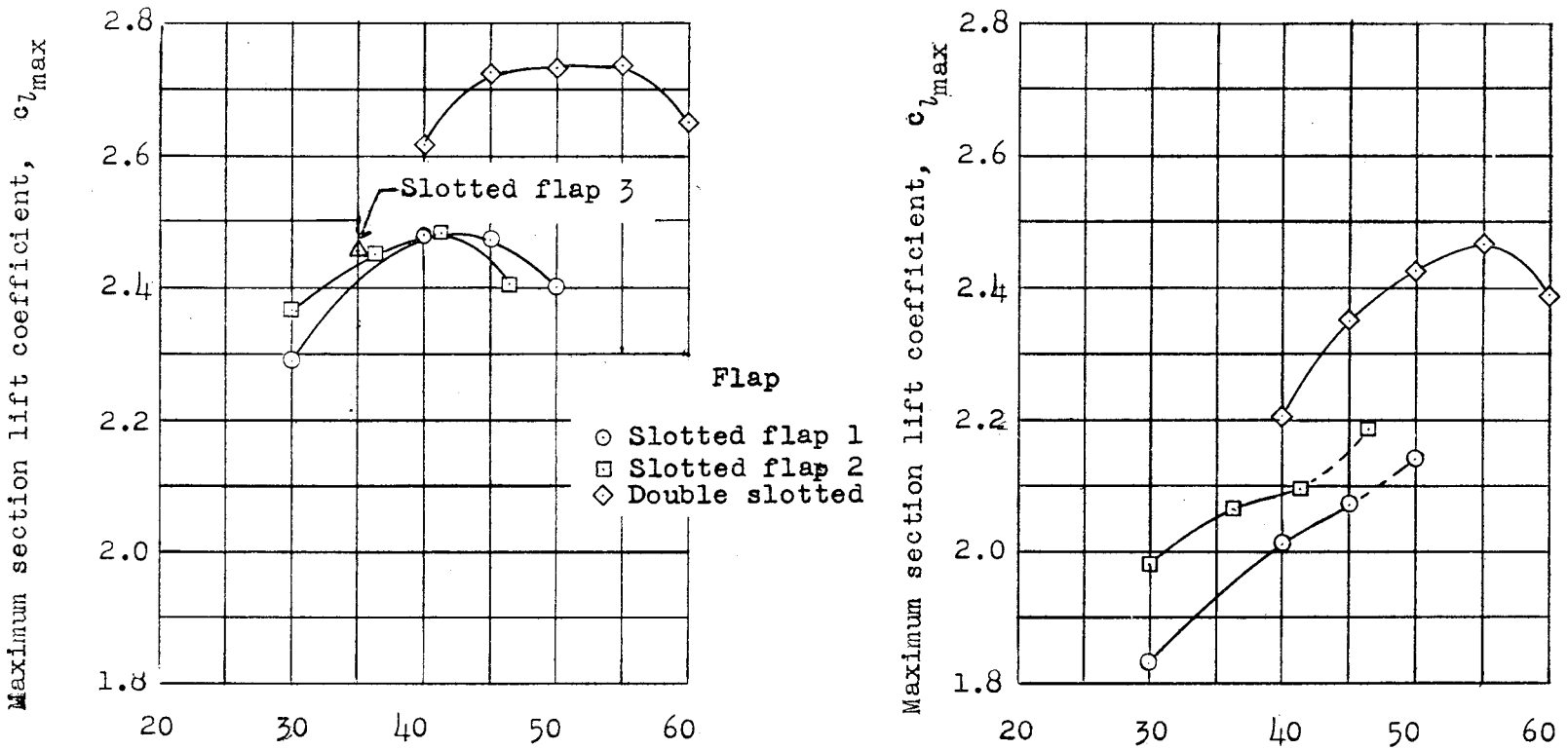

NATIONAL ADVISORY COMMITTEE FOR AERONAUTICS

(a) Surface smooth.

(b) Standard leading edge roughness.

Figure 22.- Comparison of optimum maximum lift coefficients of 65-210 airfoil section with various types of flap. $R = 6 \times 10^6$.